

Original Article

Linc00662 m⁶A promotes the progression and metastasis of pancreatic cancer by activating focal adhesion through the GTF2B-ITGA1-FAK pathway

Shuo Zhang^{1,2*}, Tiantian Lai^{1,2*}, Xiaowen Su^{1,2*}, Yong Zhang¹, Junjing Zhou¹, Changyong Zhao¹, Minfeng Liu¹, Wuqiang Chen¹, Shuming Xiong¹, Yue Tao¹, Youzhao He¹, Hao Hu^{1,2,3,4,5}

¹Hepatobiliary and Pancreatic Surgery, Affiliated Hospital of Jiangnan University, 1000 Hefeng Rd, Binhu District, Wuxi 214122, Jiangsu, China; ²School of Medicine, Jiangnan University, Wuxi 214122, Jiangsu, China; ³Hepatobiliary and Pancreatic Surgery, The Third Hospital Affiliated to Nantong University, Wuxi 214041, Jiangsu, China; ⁴Medical School, Nantong University, Nantong 226001, Jiangsu, China; ⁵Wuxi Institute of Hepatobiliary Surgery, Wuxi 214122, Jiangsu, China. *Equal contributors.

Received February 2, 2023; Accepted April 21, 2023; Epub May 15, 2023; Published May 30, 2023

Abstract: Recurrence and metastasis are major factors associated with the poor prognosis of pancreatic cancer (PC). Previous studies have indicated that METTL3-mediated N6-methyladenosine (m⁶A) modification is closely associated with PC progression and prognosis. However, its underlying regulatory mechanisms remain unclear. In this study, we found that METTL3 was upregulated in PC tissues and cells and was associated with malignant tumor progression and poor progression-free survival in PC. Linc00662 was screened as a m⁶A-enriched RNA that promoted tumor growth and metastasis in PC cells and mouse models and was associated with poor clinical prognosis. Four m⁶A motifs were identified in Linc00662, which maintained the stability of Linc00662 in an IGF2BP3-coupled manner and were closely associated with the pro-tumor properties of Linc00662 *in vitro* and *in vivo*. ITGA1 was identified as a downstream gene regulated by Linc00662. Linc00662 recruits GTF2B to activate the transcription of ITGA1 in a m⁶A-dependent manner and initiates the formation of focal adhesions through the ITGA1-FAK-Erk pathway, thereby promoting malignant behavior in PC cells. The FAK inhibitor-Y15 obviously repressed tumor progression in Linc00662-overexpressing PC cells *in vitro* and *in vivo*. This study proposes a novel regulatory mechanism of Linc00662 in oncogene activation in PC and indicates that Linc00662 and its downstream genes are potential targets for PC therapy.

Keywords: Pancreatic cancer, N6-methyladenosine, Linc00662, focal adhesion, ITGA1, FAK

Introduction

Pancreatic cancer (PC) is one of the most aggressive cancers of the digestive system and is characterized by late diagnosis and poor prognosis [1-3]. Recurrence and metastasis are major factors associated with the poor prognosis of PC, which cannot be controlled with current therapeutic strategies. In most patients, chemotherapy is the only option despite widespread chemoresistance. Therefore, precision medicine and targeted therapies represent promising novel therapeutic strategies [4]. However, only a limited number of functional targets of PC and their underlying mechanisms have been identified.

Epigenetic modifications such as RNA modifications are involved in carcinogenesis. Among them, N6-methyladenosine (m⁶A) is the most abundant epigenetic modification of RNA. m⁶A methylation is catalyzed at the N6 position of RNA molecules by the effector proteins, including enzymes such as the “writers” (METTL3, METTL14, and WTAP) [5, 6] and “erasers” (FTO and ALKBH5), which effectively install and remove RNA methylation [7, 8]. After m⁶A modification, mature RNAs are exported from nuclei to cytoplasm where they are recognized by different “readers” (HNRNPC, YTHDF1/2/3 and IGF2BP1/2/3) [9, 10].

METTL3 was originally identified as a methyltransferase responsible for m⁶A modification

Table 1. The clinicopathological information of 30 patients with PC

Characteristics	
Age (year, mean ± SD)	66.47±8.60
Gender (n, male/female)	17/13
Pathological grade (n/%)	
G1-G2/G2	22/73.33%
G2-G3/G3	8/26.67%
Clinical stage (n/%)	
I	15/50.00%
II/III	15/50.00%
Lymph node metastasis (n/%)	
N0	18/60.00%
N1/N2	12/40.00%
Nerve invasion (n/%)	
Yes	21/70.00%
No	9/30.00%
Vascular invasion (n/%)	
Yes	8/26.67%
No	22/73.33%
Distant metastasis (n/%)	
Yes	0/0.00%
No	30/100.00%

[11, 12], which plays different roles in tumor progression depending on the tumor type. It has been reported that METTL3 promotes the translation of oncogenes such as EGFR, TAZ, and WTAP, and promotes malignant growth in breast and lung cancers [13, 14]. In contrast, METTL3 inhibited tumor growth in renal cell carcinoma and glioblastoma [15, 16]. Previous studies have identified several m⁶A regulators that are closely related to overall survival in PC, including the METTL3, IGF2BPs family, and HNRNPC [17, 18]. It has been reported that METTL3 expression is upregulated in PC tissues compared to that in paracancerous tissues, which enhances the proliferative, invasive, and migratory capacities [19] and promotes chemoresistance and radioresistance in PC cells [20]. In addition, high METTL3 levels predict poor prognosis in patients with PC [17]. These results indicate that METTL3 plays an oncogenic role in PC, however the underlying mechanisms remain unclear.

Long non-coding RNA (lncRNAs) are an abundant and functionally diverse set of non-coding RNA (> 200 nt transcripts) that show limited or no protein-coding capacity [21, 22], while playing critical roles in the malignant progression of cancer [23, 24]. Several studies have reported that m⁶A in lncRNAs is involved in tumor pro-

gression and metastasis [25, 26]. In hepatocellular carcinoma, m⁶A modification induces the upregulation of Linc00958, which subsequently promotes tumor metastasis through the miR-3619-5p/HDGF axis [25]. In lung cancer, the lncRNA THOR plays an oncogenic role in a m⁶A-dependent manner [26]. In prostate cancer, the lncRNA NEAT1 promotes bone metastasis through m⁶A modifications [27].

These findings indicate that m⁶A modification may play a vital role in the malignant progression and metastasis of PC. Therefore, it is important to explore the m⁶A profiles of the PC. This study aimed to identify m⁶A-enriched lncRNAs in PC and elucidate the underlying mechanisms of tumor progression and metastasis, which will aid in identifying potential novel molecular targets to optimize current therapeutic strategies and improve the clinical prognosis of patients with PC.

Materials and methods

Patients and tissue samples

Fresh tumor tissues and paired adjacent non-tumor tissue samples were collected from 30 patients with PC who underwent surgical resection between June 2021 and May 2022 at the Affiliated Hospital of Jiangnan University. None of the patients underwent preoperative chemotherapy or radiotherapy. The collected tissue samples were preserved in liquid nitrogen. The patients were followed up until August 2022. The clinicopathological information of patients is presented in **Table 1**. This study was approved by the ethics review board of the Affiliated Hospital of Jiangnan University. Signed informed consent was obtained from all patients.

RNA microarray

Three pairs of PC and adjacent non-tumor tissues were collected for RNA microarray analysis. Total RNA was extracted, amplified, and labeled with Cy3-CTP after quality assessment. Next, Cy3-labeled target was hybridized to the microarrays (KanchenBio, H1602063) for 14 h. The microarrays were scanned, and the raw signal intensities were collected for analysis.

Bioinformatic analysis

The PC gene expression array was obtained from the Gene Expression Omnibus (GEO) dataset (GDS4103, 39 pairs of PC tis-

Linc00662 m⁶A promotes PC progression

sues) to analyze the expression patterns of METTL3 and Linc00662. Correlations between gene expressions were analyzed using an online bioinformatics analysis tool (GEPIA).

Cell culture

Human pancreatic cancer cell lines (PANC-1, BxPC-3, Mia-PaCa2, Colo357, CFPAC-1) and human pancreatic ductal epithelial cell line (HPNE) were cultured in DMEM (Wisent, Shanghai, China) supplemented with 10% fetal bovine serum (Wisent, Shanghai, China). All cell lines used in this study were mycoplasma-free and were authenticated using STR in the last three years.

Quantitative PCR (qPCR)

Total RNA was extracted from tissues and cells using TRIzol reagent (Invitrogen, Carlsbad, CA, USA), according to the manufacturer's instructions. Total RNA was reverse transcribed using a reverse transcription kit (ProteinBio, Nanjing, China) according to the manufacturer's instructions. SYBR Green qPCR Supermix (ProteinBio, Nanjing, China) was used for the qPCR analysis. β -actin was used to normalize the RNA levels using the $2^{-\Delta\Delta Ct}$ method. The primer sequences used for qPCR are listed in [Supplementary Table 1](#).

Stable cell line construction

A lentivirus encoding a small hairpin RNA (shRNA) targeting METTL3 was constructed by GeneChem (Shanghai, China) (targeting sequence: sh-1 5'-CAGCTTCAGCAGTTCCTGAT-3', sh-2 5'-ATGCACATCCTACTCTTGTA-3', sh-3 5'-GTGCAGAACAGGACTCGACTA-3'). A plasmid encoding shRNA targeting Linc00662 was constructed by ProteinBio (Nanjing, China). Plasmids encoding the wide-type Linc00662 (Linc00662 Wt) and 4A-mutated Linc00662 (Linc00662 Mut) were constructed by MiaolingBio (Wuhan, China). The cells (2×10^4) were seeded in 24-well plates. After 24 h of culture, the cells were infected with lentiviruses at a multiplicity of infection of 20 or transfected with 5 μ g of plasmids using 2.5 μ L of Lipofectamine 3000 (ThermoFisher Scientific, Massachusetts, USA). Stable cell clones were selected for 1 week using puromycin (0.5 μ g/mL) (MCE, New Jersey, USA). Efficiency was analyzed using qPCR. The primer sequences

used for qPCR are listed in [Supplementary Table 1](#).

RNA interference and plasmid transfection

Cells (6×10^5) were seeded in a 6-well plate and reached ~80% confluence after 24 h of culture. For RNA interference, a mixture of 50 nM siRNA and 7.5 μ L Lipofectamine 3000 was incubated at room temperature for 20 min and then added to the cells. For plasmid transfection, a mixture of 15 μ g plasmid and 7.5 μ L of Lipofectamine 3000 was incubated at room temperature for 20 min and then added to the cells. The cells were collected after 48 h of culture. The siRNAs used in this study are listed in [Supplementary Table 2](#).

Methylated RNA immunoprecipitation-sequencing and RNA sequencing

To determine the m⁶A modifications of individual genes in PC cells, METTL3-knockdown PANC-1 cells and negative control (NC) cells were constructed and analyzed using Methylated RNA immunoprecipitation (MeRIP) assay and RNA sequencing by GeneChem (Shanghai, China).

Methylated RNA immunoprecipitation-qPCR

To determine the m⁶A motifs on Linc00662, MeRIP-qPCR was performed with a Magna MeRIP[™] m⁶A kit (Merck, Germany) according to the manufacturer's instructions. The collected solutions were subjected to qPCR. Primers used in this study are listed in [Supplementary Table 1](#).

Protein isolation and western blotting

Total protein was extracted from the cells using radioimmunoprecipitation assay lysis buffer (Beyotime, Suzhou, China). The protein extracts were separated on 10% gels via sodium dodecyl sulfate-polyacrylamide gel electrophoresis (SDS-PAGE) and then transferred to 0.45 nm polyvinylidene difluoride (PVDF) membranes (Millipore, Massachusetts, USA). The proteins were probed with specific antibodies after the blot was blocked with a blocking buffer (Beyotime, Haimen, China). Protein expression was visualized using Super ECL Chemiluminescent Substrate Kit (Millipore, Massachusetts, USA). The antibodies used in this study are listed in [Supplementary Table 3](#).

Linc00662 m⁶A promotes PC progression

Fluorescence in situ hybridization (FISH)

Specific FISH probes for Linc00662 were designed and synthesized by GenePharma (Suzhou, China). Hybridization was performed in PC cells using the RiboTM Fluorescent In Situ Hybridization Kit (Ribo, Guangzhou, China). Briefly, the cells were fixed with 4% paraformaldehyde (PFA) solution for 10 min. After permeation, the cells were blocked with pre-hybridization solution at 37°C for 30 min. They were then hybridized with FISH probes overnight at 37°C. Finally, the cells were washed and counterstained with DAPI. The cells were examined using a confocal laser scanning microscope (Leica Microsystems, Mannheim, Germany). The FISH probe mix sequences for Linc00662 were as follows: GAGCG+TCCCTGTGCGAGG+TC TAGAGGGGC+CCGTAGAGGAGGGACCTCACCAG T+TTCAGAAGCG+TGTAGGCAC.

Immunofluorescence

The cells were fixed in 4% PFA solution for 10 min. After blocking, the cells were incubated with the primary antibody overnight at 4°C. The membranes were then incubated with the secondary antibody for 1 h at room temperature. Finally, the cells were counterstained with YF488-Phalloidin (Proteinbio, Nanjing, China) and DAPI (Beyotime, Haimen, China). Cells were stored in the dark at 4°C until further investigation. Protein expression was quantitatively analyzed using the ImageJ software (National Institutes of Health, Bethesda, USA). The antibodies used in this study are listed in [Supplementary Table 3](#).

Cell counting kit-8 assay

Cell proliferation was detected using the cell counting kit-8 (CCK8) kit (MCE, New Jersey, USA). Briefly, the cells were seeded in 96-well plates (2×10^3 cells/well) and inoculated with complete medium at 37°C with 5% CO₂ for 96 h. 10 µL of CCK8 reagent and 90 µL of complete medium were mixed and added to each well every 24 h and incubated at 37°C for 2 h. The plates were analyzed using a microplate reader at an OD450.

Clone formation assay

The cells were seeded in 6-well plates (500 cells/well) and incubated with complete medi-

um at 37°C with 5% CO₂, and the medium was replaced every 3-4 days. After 2 weeks, the colonies were fixed in 4% PFA solution for 20 min, and stained with 0.1% crystal violet solution for 30 min.

Wound-healing assay

Cells were seeded in 6-well plates and cultured until confluence. A wound was inflicted using a 200 µL pipette tip. The cells were washed with PBS to remove the detached cells and cultured in a serum-free medium. Images were taken at 0 h and 24 h using a microscope. The area of the wound was measured using the ImageJ software.

Transwell assay

Cell migration assays were performed as follows. Cells (20,000-50,000 cells/well) suspended in serum-free medium were placed into the upper chamber (Corning, 3422, USA), and culture medium supplemented with 10% FBS was added to the lower chamber. The plates were incubated at 37°C with 5% CO₂ for 24 h. The cells in the top chamber were removed using a cotton swab. The cells on the lower membrane surface were fixed in 4% PFA solution for 20 min, and stained with 0.1% crystal violet for 30 min. The membrane was then dried and observed under a microscope. Cells in five random fields of view were counted at 100 × magnification. For the invasion assay, the experimental procedures were similar to those used for the migration assay, except that the upper chambers were coated with Matrigel (BD Biosciences, USA).

RNA decay assays

To assess RNA stability, the half-life of Linc00662 was measured. Briefly, cells were treated with 5 µg/mL actinomycin D (Sigma-Aldrich, USA). Next, the cells were harvested at different time points to extract RNA using TRIzol reagent for qPCR. The half-life of the Linc00662 was calculated, and β-actin was used to normalize the data. The primers used in this study are listed in [Supplementary Table 1](#).

RNA pull-down

A biotin-labeled RNA probe targeting Linc00662 (probe sequence: AGTCTGTAAGTGGCCTGGAT-

GCTC) was synthesized by GenePharma (Suzhou, China). RNA pull-down assays were performed using the Pierce™ magnetic RNA-protein pull-down kit (Thermo Scientific, USA) according to the manufacturer's instructions. Briefly, biotin-labeled RNA probes were incubated with magnetic beads for 1 h at room temperature. Next, cell lysates were harvested and incubated with magnetic beads for 3 h at 4°C. Enriched proteins were subjected to SDS-PAGE for western blot analysis or mass spectrometry (Nanjing Medical University).

RNA immunoprecipitation (RIP)

RNA immunoprecipitation (RIP) was performed using a Magna RIP RNA-Binding Protein Immunoprecipitation Kit (Millipore, Billerica, MA, USA) according to the manufacturer's instructions. Briefly, cells were collected and lysed with RIP lysis buffer. Magnetic beads were incubated with IGF2BP3 or GTF2B antibodies for 1 h at room temperature. IgG was used as a negative control. After washing, the beads were incubated with cell lysis at 4°C for 3 h. The beads were then collected and washed, and the RNA complexes were isolated by phenol-chloroform extraction. Enriched RNA fragments were subjected to qPCR analysis.

Dual-luciferase reporter assay

A dual-luciferase reporter vector with the promoter of ITGA1 and a plasmid encoding GTF2B were constructed by MiaolingBio (Wuhan, China). Cells (6×10^5) were seeded in a 6-well plate and reached ~80% confluence after 24 h of culture. Plasmids and dual-luciferase reporter vector were cotransfected into cells at a ratio of 2:1 (6:3 µg) using 5 µL of Lipofectamine 3000. Luminescence units were measured using a dual-luciferase reporter assay kit (ProteinBio, Nanjing, China) according to the manufacturer's instruction. Briefly, the cells were collected after 48 h of culture in a lysis buffer. Firefly luciferase (Fluc) and Renilla luciferase (Rluc) levels were measured using a luminescence reader by sequentially adding individual substrates. The relative luminescence units (RLU) were calculated as Fluc/Rluc.

Xenograft model and in vivo metastasis assay

Four-week-old female BALB/c nude mice (18-20 g) were housed in an SPF facility with a

12/12 h day/night cycle and free access to chow and water. The animal study was approved by the Ethics Committee of the Laboratory Animal Management of Jiangnan University. The animals were terminated if the body weight loss was more than 20-25% or the tumor weight was over 10% of the body weight. All the animals were euthanized.

For the tumor growth study, nude mice were subcutaneously inoculated into the flanks with PC cells (3×10^6) suspended in 0.1 mL PBS. Tumor volumes were calculated as $1/2$ (length \times width²) weekly. After 4 weeks, the xenograft tumors were harvested for analysis. To examine the role of the FAK inhibitor in tumor growth, nude mice were inoculated subcutaneously into the flanks with 3×10^6 stable cells suspended in 0.1 mL PBS. After 1 week, pre-established tumor xenografts were treated with Y15 (0.5 mg/kg, 2 \times /week \times 3) (MCE, New Jersey, China). After another 3 weeks, the xenograft tumors were harvested for analysis.

In the metastasis model, PC cells (2×10^6) in 0.1 mL PBS were injected into nude mice through their tail veins. Six weeks later, the lungs were removed for the evaluation of lung metastasis using hematoxylin and eosin (H&E) staining.

Hematoxylin and eosin staining

The lung tissues were stained with hematoxylin and eosin (H&E) staining. Briefly, the paraffin-embedded sections were de-waxed in xylene and rehydrated using a graded alcohol series. Sections were incubated with hematoxylin for 5 min followed by a differentiation solution for 30 s. After washing with water, sections were dipped in eosin for 2 min.

Adhesion assay

PC cells (1×10^4) were seeded in 96-well plates which were precoated with 10 µg/mL collagen (MCE, New Jersey, USA) overnight at 37°C. After incubation at 37°C for 1 h, cells that did not adhere to the plates were washed off with PBS. Adherent cells were fixed in 4% PFA for 10 min, stained with 0.1% crystal violet for 30 min. The cells in four random fields of view were counted at 100 \times magnification.

Cell spreading assay and immunofluorescence microscopy

The cell spreading assay was performed as previously described with some modifications. Cell culture dishes (2 cm) were precoated with 10 µg/mL collagen (MCE, New Jersey, USA) overnight at 37°C, followed by blocking with 1% BSA. The cells (2×10^4) were seeded in the dishes and incubated at 37°C. After 1 h, the cells were fixed in 4% PFA for 10 min, permeabilized with 0.2% Triton X-100 for 15 min, and blocked with 5% BSA for 2 h. For staining, the cells were incubated with the primary antibody overnight at 4°C and then incubated with the secondary antibody for 1 h at room temperature. Finally, the cells were counterstained with YF488-Phalloidin (Proteinbio, Nanjing, China) and DAPI. The cells were stored in the dark at 4°C until further investigation. The antibodies used in this study are listed in [Supplementary Table 3](#).

Statistical analysis

Statistical analyses were performed using GraphPad Prism (version 6.0). Quantitative data are expressed as mean \pm standard deviation. Differences between the two groups were analyzed using Student's t-test. Categorical data were analyzed using χ^2 -test or Fisher's exact test. Statistical significance was set at a $P < 0.05$.

Results*Upregulated METTL3 was associated with disease progression and poor prognosis in patients with PC*

Differentially expressed genes (DEGs) between three pairs of PC tumor and adjacent non-tumor tissues were identified using RNA microarray under the criteria of $P < 0.05$, false discovery rate (FDR) < 0.05 and fold change (FC) ≥ 2 . We identified 8345 DEGs (5131 up-regulated DEGs and 3214 down-regulated DEGs), among which, METTL3 was upregulated in PC tissues compared to adjacent tissues (FC = 2.991, $P = 0.001$, FDR = 0.028) (**Figure 1A**). Next, METTL3 expression was analyzed in 39 pairs of PC tissues based on the GEO dataset (GDS4103), and the results showed that METTL3 mRNA expression was higher in PC tissues than in the adjacent normal tissues ($P = 0.000$) (**Figure 1B**).

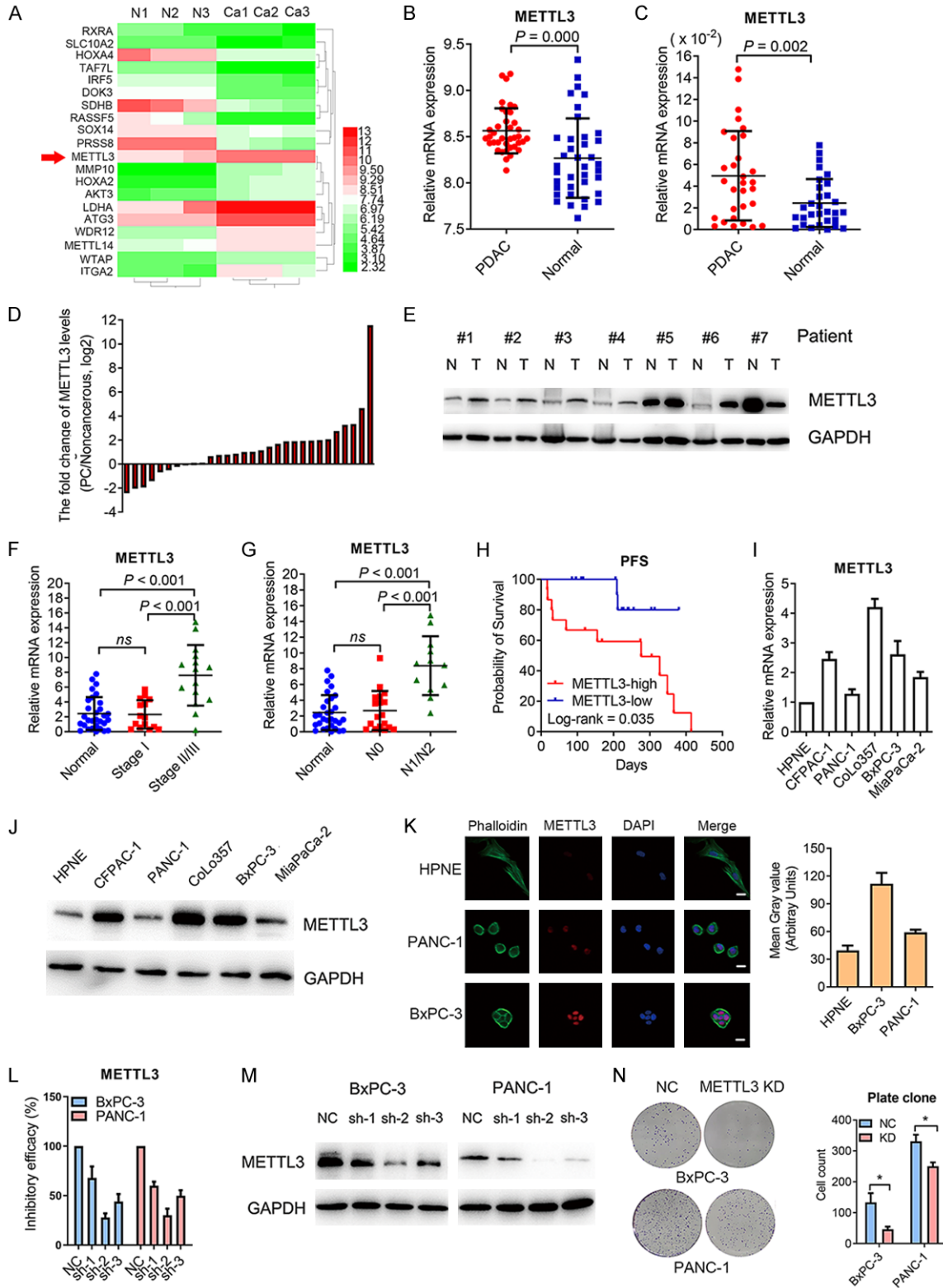
To confirm the expression level of METTL3 in PC tissues, we analyzed the expression of METTL3 in 30 pairs of PC tissues collected from our hospital and found that METTL3 mRNA was higher in PC tissues than in the adjacent tissues ($P = 0.002$) (**Figure 1C**), and more than half of PC tissues (16 out of 30 tissues, 55.0%) had two-fold higher METTL3 expression than the adjacent tissues (**Figure 1D**). Western blotting confirmed the protein levels of METTL3 in PC and adjacent tissues, which were consistent with the mRNA levels (**Figure 1E**). In the subcategory analysis of the 30 pairs of PC tissues, we found that METTL3 mRNA levels were higher in stage II/III PC tissues than in stage I PC tissues ($P < 0.001$) (**Figure 1F**), and METTL3 mRNA levels were higher in PC tissues with lymph node metastasis (N1/N2) than in PC tissues without lymph node metastasis (N0) ($P < 0.001$) (**Figure 1G**). By August 2022, there were seven deaths, five metastases and one recurrence in 30 patients with PC, yielding a median progression-free survival (PFS) of 209 days (17-414 days). The Kaplan-Meier survival curve indicated a negative association between METTL3 mRNA expression and PFS ($P = 0.035$) (**Figure 1H**). These findings revealed that higher METTL3 expression indicates more advanced disease and poor prognosis in patients with PC.

METTL3 promoted the malignant behaviors in PC cells

Next, we examined the expression of METTL3 in PC cells and found that METTL3 was upregulated in PC cells compared to that in the pancreatic epithelial cell line (HPNE) at both the mRNA and protein levels (**Figure 1I, 1J**). BxPC-3 and PANC-1 cells were used in this study. Immunofluorescence assays confirmed that METTL3 was localized in the nuclei of PC and HPNE cells, and the fluorescence intensity of PC cells was higher than that of HPNE cells (**Figure 1K**).

To examine the role of METTL3 in PC malignance, a loss-of-function assay was performed by infecting BxPC-3 and PANC-1 cells with METTL3 shRNA lentivirus to establish METTL3-knockdown cell lines. Western blotting and qPCR confirmed that METTL3-sh2 showed the highest inhibitory efficacy (**Figure 1L, 1M**), which was used for the following study. We found that the knockdown of METTL3 in PC cells repressed the number of clones formed

Linc00662 m⁶A promotes PC progression



Linc00662 m⁶A promotes PC progression

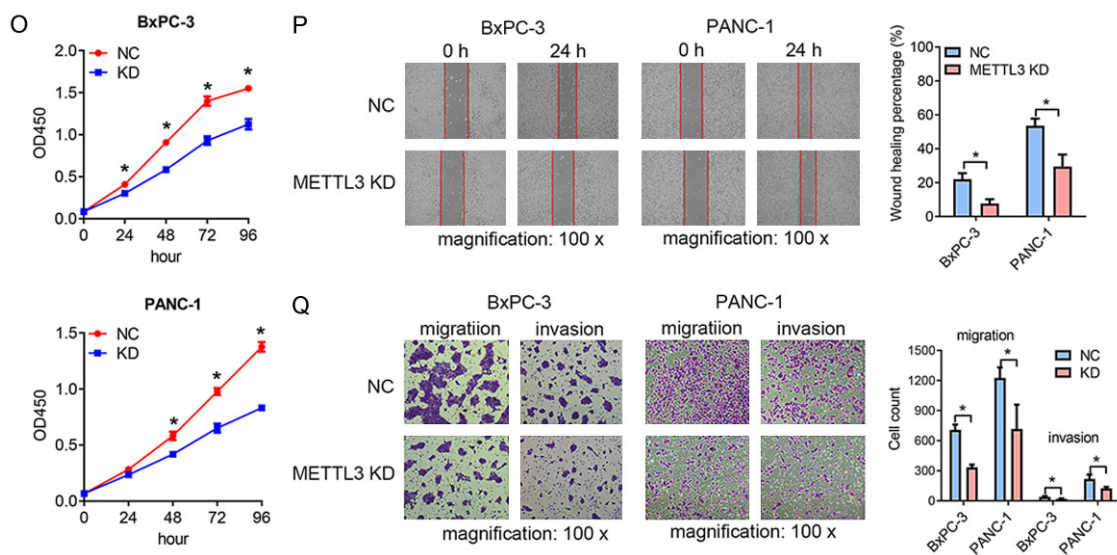


Figure 1. Upregulated METTL3 was associated with the malignant progression and poor prognosis in PC. A. METTL3 mRNA levels were upregulated in PC tissues compared to adjacent tissues (FC = 2.991, $P = 0.001$, FDR = 0.028) using RNA microarray (3 pairs of PC and adjacent tissues). B. METTL3 mRNA levels were higher in PC tissues than in the adjacent normal tissues ($P = 0.000$) based on the GEO database (GDS4103, 39 pairs of PC tissues). C. METTL3 mRNA was higher in PC tissues than in the adjacent tissues ($P = 0.002$) in 30 pairs of PC tissues collected from our hospital. D. More than half of PC tissues (16 out of 30, 55.0%) had two-fold higher METTL3 mRNA levels than the adjacent tissues. E. The protein expression of METTL3 was examined in seven pairs of PC tissues by western blotting. The protein levels of METTL3 in PC tissues were higher than in the adjacent tissues, which were consistent with the mRNA levels. F. In the subcategory analysis of the 30 pairs of PC tissues, METTL3 mRNA levels were higher in stage II/III PC tissues than in stage I PC tissues ($P < 0.001$). G. In the subcategory analysis of the 30 pairs of PC tissues, METTL3 mRNA levels were higher in PC tissues with lymph node metastasis (N1/N2) than in PC tissue without in lymph node metastasis (NO) ($P < 0.001$). H. The Kaplan-Meier survival curve indicated a negative association between METTL3 mRNA expression and PFS ($P = 0.035$). I. METTL3 expression was examined in PC cells and HPNE cells using qPCR. The results showed that METTL3 expression was higher in PC cells than in HPNE cells. J. METTL3 expression was examined in PC cells and HPNE by western blotting. The results showed that METTL3 expression was higher in PC cells than in HPNE cells. K. The immunofluorescence assays confirmed that METTL3 levels were significantly higher in PC cells than in HPNE cells. The bar chart was the quantitative analysis of the fluorescence intensity of METTL3. Scale bar: 20 μm . L. METTL3-knockdown cell lines were established by infected PC cells with METTL3 shRNA lentivirus (sh-1, sh-2, and sh-3). The inhibitory efficacy was examined using qPCR and the results showed that METTL3-sh2 showed the highest inhibitory efficacy. M. METTL3-knockdown cell lines were established by infected PC cells with METTL3 shRNA lentivirus (sh-1, sh-2, and sh-3). The inhibitory efficacy was examined by western blotting and the results showed that METTL3-sh2 showed the highest inhibitory efficacy. N. The clone formation assay indicated that the knockdown of METTL3 reduced the number of clone formation of PC cells. Representative images were displayed and the bar charts showed the differences of clone number between METTL3-knockdown PC cells and NC cells. *: $P < 0.05$. O. The CCK8 assay indicated that the knockdown of METTL3 reduced the proliferative capacity of PC cells. *: $P < 0.05$. P. The wounding healing assay indicated that the knockdown of METTL3 reduced the migratory capacity of PC cells. Representative micrographs were displayed and the bar charts showed the differences of migratory area between METTL3-knockdown PC cells and control cells. *: $P < 0.05$ magnification: 100 \times . Q. The transwell assay indicated that the knockdown of METTL3 reduced the migratory and invasive capacity of PC cells and fewer PC cells migrated/invaded to the lower side of the membrane. Representative micrographs were displayed and the bar charts showed the differences of migrated or invaded cell numbers between METTL3-knockdown PC cells and control cells. *: $P < 0.05$, magnification: 100 \times . Abbreviations: PC: pancreatic cancer, NC: negative control, KD: knockdown, CCK8: cell counting kit-8, qPCR: quantitative polymerase chain reaction, HPNE: pancreatic epithelial cell line, GEO: Gene Expression Omnibus database.

(Figure 1N) and cell viability (Figure 1O) compared to control cells. And the knockdown of METTL3 in PC cells delayed wound healing (Figure 1P) and inhibited their migratory and invasive capacities (Figure 1Q) compared to control cells. These results indicated that METTL3 promotes the malignant progression of PC.

Linc00662 was enriched with m⁶A methylation regulated by METTL3

To elucidate how m⁶A methylation is involved in tumor progression and metastasis in PC, we performed methylated RNA immunoprecipitation (MeRIP) sequencing of METTL3-knockdown PANC-1 and control cells. The results

showed that the knockdown of METTL3 dramatically reduced the number of unique m⁶A genes (Figure 2A) and m⁶A peaks (Figure 2B), resulting in 4631 hypomethyladenosine RNAs and 3151 hypermethyladenosine RNAs. By screening for lncRNAs, five hypomethyladenosine lncRNAs were identified: OIP5-AS1, AC021078.1, MAGI2-AS3, MIR100HG, and Linc00662 (Figure 2C). Furthermore, RNA sequencing revealed that the knockdown of METTL3 caused 938 downregulated RNAs and 761 upregulated RNAs (Figure 2D), and the five hypomethyladenosine lncRNAs screened by MeRIP-sequencing were all downregulated at RNA level (Figure 2E). We examined the expression of the five lncRNAs in PC cells using qPCR and found that Linc00662 showed a consistent trend in PANC-1 and BxPC-3 cells (Figure 2F). In addition, correlation analysis indicated a positive relationship between METTL3 and Linc00662 expressions in PC tissues ($P = 2.1e-08$) (Figure 2G).

Next, we analyzed the m⁶A peak on Linc00662 and found that the m⁶A peak was located on chromosome 19 (27723041~27732875) which is consistent with the Linc00662-201 transcript (Figure 2H). Further analysis showed that the m⁶A peak was localized in the third exon (exon 3) of Linc00662 containing four m⁶A motifs: A341, A672, A841 and A1725 (Figure 2I). In addition, m⁶A motifs were predicted using the online tool SRAMP (a sequence-based N⁶-methyladenosine (m⁶A) modification site predictor). Three of the four m⁶A motifs were covered with moderate or low confidence (Figure 2J). Finally, a MeRIP-qPCR assay was performed, which verified that there were four m⁶A motifs in Linc00662 (Figure 2K).

Linc00662 mediated the malignant progression and metastasis of PC in a m⁶A-dependent manner

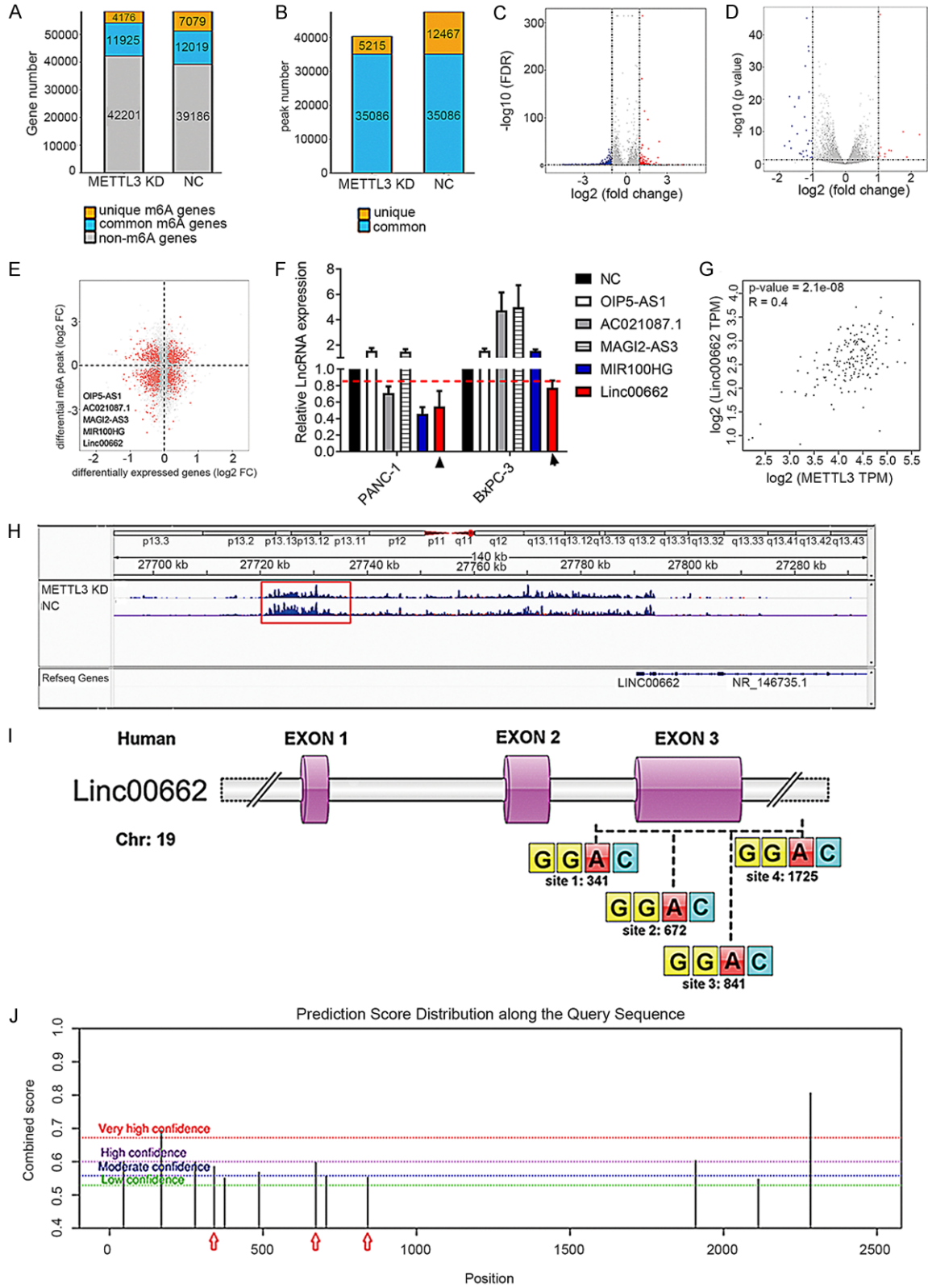
To examine the role of Linc00662 in PC, we first analyzed Linc00662 expression in PC tissues. The results showed that Linc00662 was significantly upregulated in PC tissues according to GEO dataset ($P = 0.011$) (GDS4103, 39 pairs of PC tissues) (Figure 3A). In the 30 pairs of PC tissues collected from our hospital, Linc00662 was higher in PC tissues than the adjacent tissues ($P = 0.007$) (Figure 3B), and the expression level of Linc00662 was upregulated \geq two-

fold in 56.7% (17/30) of PC tissues (Figure 3C). In the subcategory analysis, Linc00662 was higher in stage II/III PC tissues than in stage I PC tissues ($P = 0.029$) (Figure 3D), and Linc00662 was higher in PC tissues with lymph node metastasis (N1/N2) than in PC tissues without lymph node metastasis (N0) ($P = 0.009$) (Figure 3E). The Kaplan-Meier survival curve indicated that high expression of Linc00662 predicted poor PFS in patients with PC ($P = 0.043$) (Figure 3F). These results indicated that Linc00662 played an oncogenic role in PC.

Next, a loss-of-function assay was conducted to examine the oncogenic properties of Linc00662 in PC cells. Linc00662-knockdown cell lines were established via shRNA plasmid transfection after screening for the most efficient siRNA targeting Linc00662 (Figure 3G). *In vitro*, we found that the knockdown of Linc00662 in PC cells inhibited cell viability (Figure 3H), delayed wound healing (Figure 3I), and repressed the invasive capacity (Figure 3J) compared to control cells. *In vivo*, cells were inoculated subcutaneously into the flanks of nude mice. After 4 weeks, xenograft tumors were harvested for evaluation (Figure 3K). The results showed that the knockdown of Linc00662 reduced subcutaneous tumor size and weight (Figure 3L, 3M). The results from the tail vein metastasis model showed that the knockdown of Linc00662 significantly reduced the area of lung-metastatic lesions (Figure 3N, 3O). These results indicated that Linc00662 promoted malignant progression and metastasis in PC.

To verify the relationship between m⁶A methylation and the oncogenic properties of Linc00662, overexpression vectors encoding wild-type Linc00662 (designated as Linc00662 Wt) and 4A-mutated Linc00662 (the adenine residues of the four m⁶A motifs, A672, A841 and A1725 were replaced by guanine residues, designated as Linc00662 Mut) were constructed. Stably overexpressing cell lines were generated, and qPCR confirmed the overexpression of Linc00662 in PC cells (Figure 4A). A gain-of-function assay was performed. *In vitro*, the results showed that the cell proliferative capacity (Figure 4B, 4C), wound healing capacity (Figure 4D) and cell invasive capacity (Figure 4E) were significantly enhanced in Linc00662 Wt cells, but not in Linc00662 Mut cells using

Linc00662 m⁶A promotes PC progression



Linc00662 m⁶A promotes PC progression

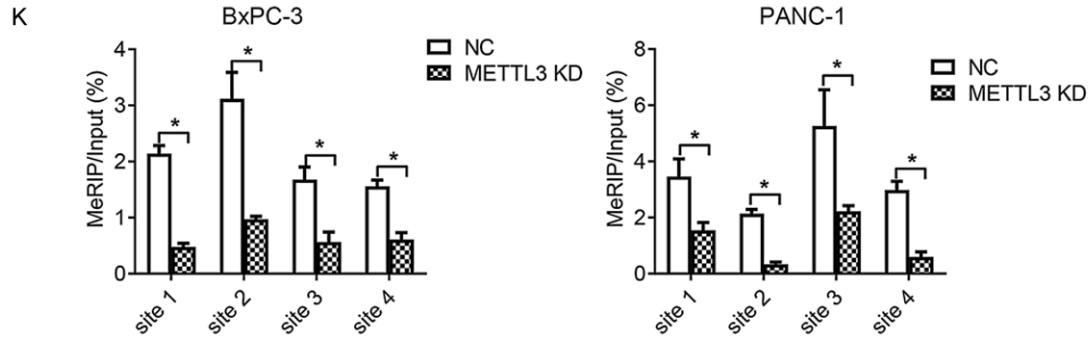
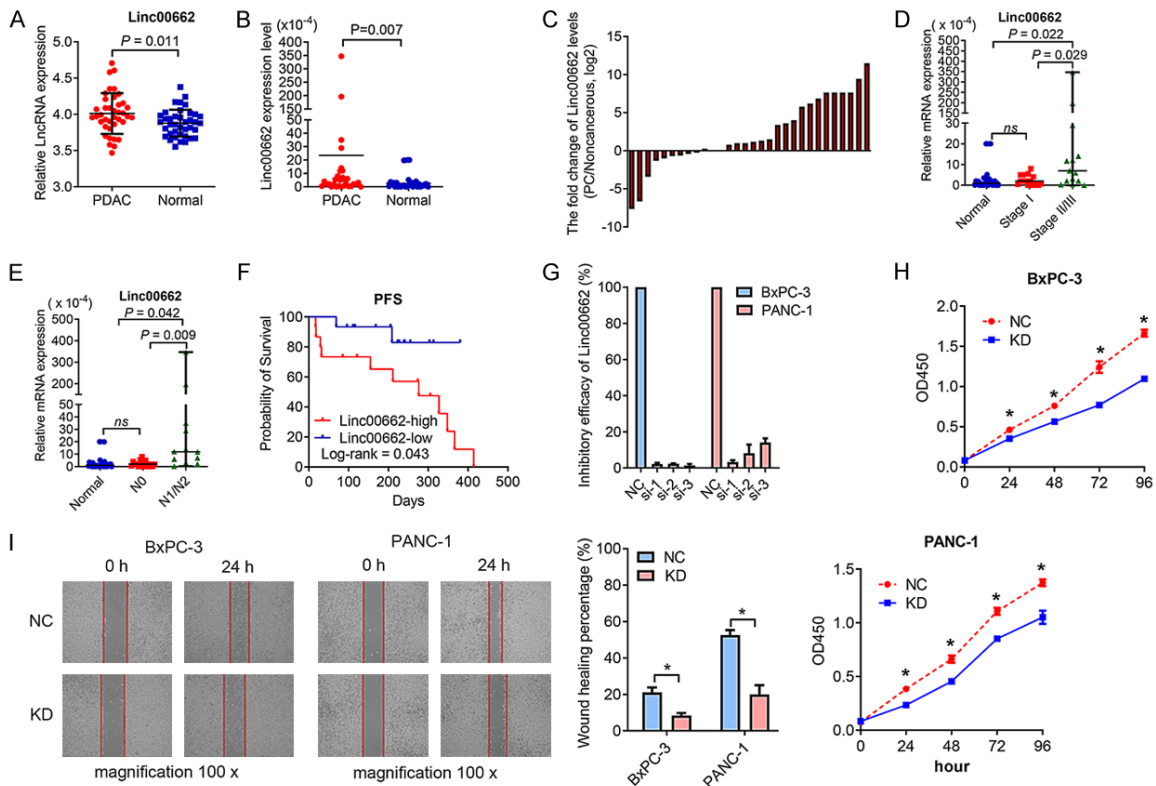


Figure 2. Linc00662 was identified as a m⁶A-enriched lncRNA in PC cells. A. MeRIP sequencing analysis showed that the knockdown of METTL3 significantly reduced the number of unique m⁶A genes in PANC-1 cells. B. MeRIP sequencing analysis showed that the knockdown of METTL3 significantly reduced the number of unique m⁶A peaks in PANC-1 cells. C. MeRIP sequencing revealed that the knockdown of METTL3 caused 4631 hypomethyladenosine RNAs and 3151 hypermethyladenosine RNAs in PANC-1 cells. D. RNA sequencing revealed that the knockdown of METTL3 caused 938 downregulated RNAs and 461 upregulated RNAs in PANC-1 cells. E. An interaction analysis of MeRIP and RNA sequencing screened five hypomethyladenosine lncRNAs (OIP5-AS1, AC021078.1, MAGI2-AS3, MIR100HG, Linc00662) in METTL3-knockdown PANC-1 cells, which were all downregulated at the RNA level. F. The expression of the five lncRNAs was examined in PC cells using qPCR and the results showed that Linc00662 showed a consistent downregulation in the two strains of METTL3-knockdown PC cells. G. Correlation analysis indicated a positive relationship between METTL3 and Linc00662 expressions in PC tissues ($P = 2.1\text{e-}08$) using an online bioinformatics analysis tool (GEPIA). H. The m⁶A peak on Linc00662 was located on chromosome 19 (27723041~27732875), which is consistent with the Linc00662-201 transcript. I. Schematic diagram of m⁶A motifs on Linc00662. The m⁶A peak was located on the third exon (exon 3) of Linc00662 containing four m⁶A motifs: A341, A672, A841, and A1725. J. The m⁶A motifs on Linc00662 were predicted using the online tool SRAMP. Three of the four m⁶A motifs were covered with moderate or low confidence. Red arrows indicate the m⁶A motifs: A341, A672, and A841. K. Four m⁶A motifs on Linc00662 were confirmed in PC cells using MeRIP-qPCR. Abbreviations: PC: pancreatic cancer, MeRIP: Methylated RNA immunoprecipitation, qPCR: quantitative polymerase chain reaction, m⁶A: N⁶-methyladenosine.



Linc00662 m⁶A promotes PC progression

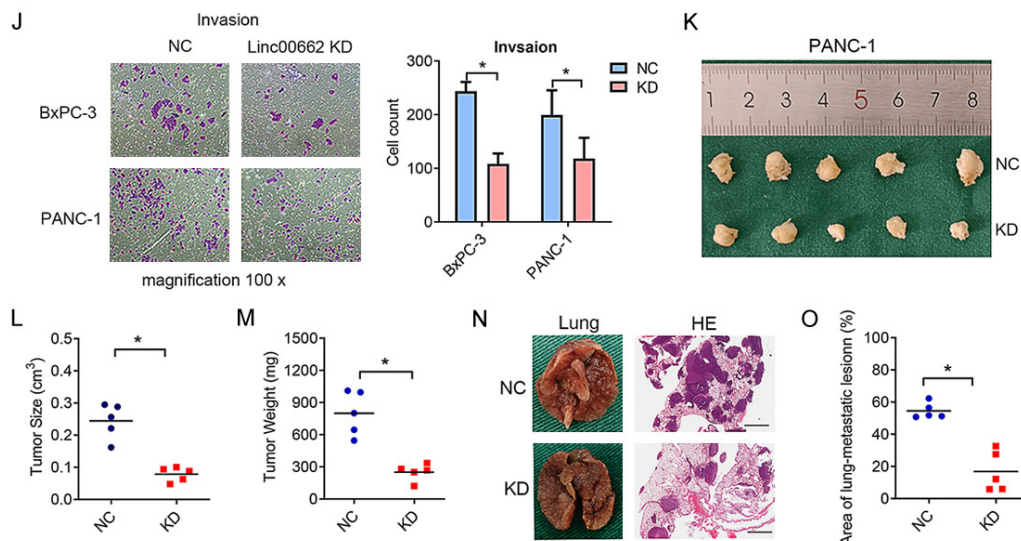


Figure 3. Upregulated Linc00662 was associated with the malignant progression and poor prognosis of PC. A. Linc00662 was significantly upregulated in PC tissues according to the GEO dataset ($P = 0.011$) (GDS4103, 39 pairs of PC tissues). B. In the 30 pairs of PC tissues collected from our hospital, Linc00662 was higher in PC tissues than the adjacent tissues ($P = 0.007$). C. In the 30 pairs of PC tissues collected from our hospital, the expression level of Linc00662 was upregulated \geq two-fold in 56.7% (17/30) of PC tissues. D. In the subcategory analysis, Linc00662 was higher in stage II/III PC tissues than in stage I PC tissues ($P = 0.029$). E. In the subcategory analysis, Linc00662 was higher in PC tissues with lymph node metastasis (N1/N2) than in PC tissues without lymph node metastasis (NO) ($P = 0.009$). F. The Kaplan-Meier survival curve indicated that high expression of Linc00662 predicted poor PFS in patients with PC ($P = 0.043$). G. Linc00662 was knocked down using siRNAs to screen for the most efficient siRNA targeting Linc00662. H. The CCK8 assay indicated that the knockdown of Linc00662 reduced the proliferative capacity of PC cells. *: $P < 0.05$. I. The wounding healing assay indicated that the knockdown of Linc00662 reduced the migratory capacity of PC cells. Representative micrographs were displayed. The bar charts showed the differences of migratory area between Linc00662-knockdown PC cells and control cells. *: $P < 0.05$ magnification: 100 \times . J. The transwell assay indicated that the knockdown of Linc00662 reduced the invasive capacity of PC cells and fewer PC cells invaded to the lower side of the membrane. Representative micrographs were displayed. The bar charts showed the differences of invaded cell numbers between Linc00662-knockdown PC cells and control cells. *: $P < 0.05$ magnification: 100 \times . K. A mouse xenograft model was used to evaluate the effect of Linc00662 on cell proliferation *in vivo*. Images of transplanted subcutaneous tumors were displayed. L. The results showed that the knockdown of Linc00662 inhibited subcutaneous tumor growth of PANC-1 cells. *: $P < 0.05$. M. The results showed that the knockdown of Linc00662 inhibited subcutaneous tumor growth of PANC-1 cells. *: $P < 0.05$. N. The effect of Linc00662 on tumor metastasis *in vivo* was evaluated in BALB/c nude mice by injecting PC cells through their tail veins. Representative images of lung removed from mouse models were displayed. H&E staining was performed to confirm the histomorphology of the metastatic lesions. Representative micrographs were displayed for cancerous lesion in the lungs detected by H&E staining. Scale bar: 2000 μ m. O. The results showed that the knockdown of Linc00662 significantly reduced the area of lung-metastatic lesions. The bar charts showed the differences of area of lung-metastatic lesions between Linc00662-knockdown PC cells and control cells. *: $P < 0.05$. Abbreviations: PC: pancreatic cancer, NC: negative control, KD: knock down, CCK8: cell counting kit-8, qPCR: quantitative polymerase chain reaction, GEO: Gene Expression Omnibus database, H&E: hematoxylin and eosin.

CCK8, colony formation, wound healing, and transwell assays. *In vivo*, we found that the overexpression of Linc00662 Wt increased subcutaneous tumor size and weight as well as the area of lung-metastatic lesions, but the overexpression of Linc00662 Mut failed (**Figure 4F-J**). Collectively, these results confirm that m⁶A methylation in Linc00662 is required to regulate the malignant progression and metastasis of PC.

IGF2BP3 maintained the stability of Linc00662 as a m⁶A reader

We further explored the role of m⁶A methylation in Linc00662. The level of Linc00662 Mut was relatively lower than that of Linc00662 Wt in PC cells (**Figure 4A**); therefore, we speculated that m⁶A modification may regulate the stability of Linc00662. We examined the half-life of Linc00662 and found that the knockdown of

Linc00662 m⁶A promotes PC progression

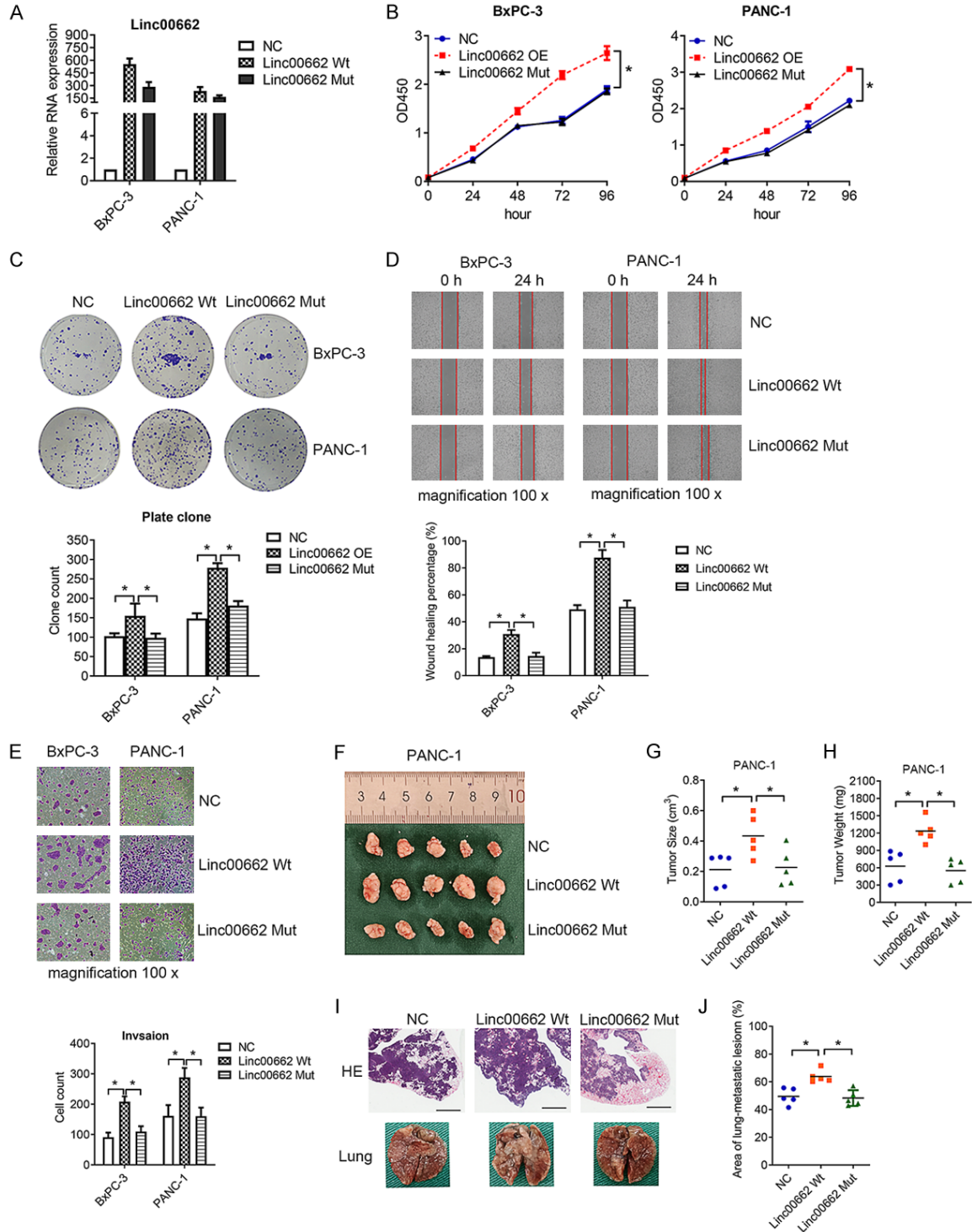


Figure 4. Linc00662 mediated the malignant progression of PC in a m⁶A-dependent manner. A. Overexpression vectors encoding Linc00662 Wt and Linc00662 Mut (the adenine residues of the four m⁶A motifs A341, A672, A841, and A1725 were replaced by guanine residues) were constructed. Stably-overexpressing cell lines were generated and qPCR confirmed the overexpression of Linc00662 in PC cells. B. The CCK8 assay showed that the cell proliferative capacity was significantly increased in Linc00662 Wt cells, but not in Linc00662 Mut cells. C. The colony formation assay showed that the cell proliferative capacity was significantly increased in Linc00662 Wt cells, but not in Linc00662 Mut cells. Representative images were displayed and the bar charts showed the differences of clone number among Linc00662 Wt cells, Linc00662 Mut cells, and control cells. *: $P < 0.05$. D. The wound healing assay indicated that the overexpression of Linc00662 Wt significantly increased cell migratory

capacity, but the overexpression of Linc00662 Mut failed. Representative micrographs were displayed and the bar charts showed the differences of migratory area among Linc00662 Wt cells, Linc00662 Mut cells, and control cells. *: $P < 0.05$, magnification: 100 ×. E. The transwell assay revealed that the overexpression of Linc00662 Wt significantly increased cell invasive capacity, but the overexpression of Linc00662 Mut failed. Representative micrographs were displayed and the bar charts showed the differences of invaded cell numbers among Linc00662 Wt cells, Linc00662 Mut cells, and control cells. *: $P < 0.05$, magnification: 100 ×. F. A mouse xenograft model was used to evaluate the effect of m⁶A on Linc00662 on cell proliferation *in vivo*. Images of transplanted subcutaneous tumors were displayed. G. The results showed that the overexpression of Linc00662 Wt in PANC-1 cells increased subcutaneous tumor size, but the overexpression of Linc00662 Mut failed. *: $P < 0.05$. H. The results showed that the overexpression of Linc00662 Wt in PANC-1 cells increased subcutaneous tumor weight, but the overexpression of Linc00662 Mut failed. *: $P < 0.05$. I. The effect of m⁶A on Linc00662 on tumor metastasis *in vivo* was evaluated in BALB/c nude mice by injecting PC cells through their tail veins. Representative images of lung removed from mouse models were displayed. H&E staining was performed to confirm the histomorphology of the metastatic lesions. Representative micrographs were displayed for cancerous lesion in the lungs detected by H&E staining. Scale bar: 2000 μm. J. The results showed that the overexpression of Linc00662 Wt in PANC-1 cells increased the area of lung-metastatic lesions, but the overexpression of Linc00662 Mut failed. The bar charts showed the differences of area of lung-metastatic lesions among Linc00662 Wt, Linc00662 Mut, and control cells. *: $P < 0.05$. Abbreviations: PC: pancreatic cancer, NC: negative control, Wt: wide type, Mut: 4A-mutated, CCK8: cell counting kit-8, MeRIP: Methylated RNA immunoprecipitation, qPCR: quantitative polymerase chain reaction, H&E: hematoxylin and eosin, m⁶A: N⁶-methyladenosine.

METTL3 in PC cells reduced the half-life of Linc00662 compared to that in control cells (**Figure 5A**). IGF2BPs (IGF2BP1/2/3) participate in RNA stabilization as m⁶A readers. We then screened the m⁶A readers of Linc00662 by RNA Pulldown/MS and found that IGF2BP3 was the only member of the IGF2BPs bound to Linc00662 (**Figure 5B-D**). To verify this, we analyzed the proteins pulled down with the Linc00662 probe by western blotting and found that IGF2BP3 was a component of the complexes (**Figure 5E**). The RIP assay verified that Linc00662 was enriched in the IGF2BP3 group but not in the IgG group (**Figure 5F**). In addition, correlation analysis showed that IGF2BP3 expression was positively related with Linc00662 expression in PC tissues ($P = 0.046$) (**Figure 5G**). These results indicated that IGF2BP3 may be the m⁶A reader of Linc00662.

To further verify the effect of IGF2BP3 on Linc00662, we knocked down IGF2BP3 in PC cells (**Figure 5H, 5I**) using siRNAs and examined its effect on the half-life of Linc00662. The results showed that the knockdown of IGF2BP3 in PC cells reduced the half-life of Linc00662 compared to that in control cells (**Figure 5J**), indicating that IGF2BP3 can maintain the stability of Linc00662. Collectively, IGF2BP3 maintains the stability of Linc00662 as a m⁶A reader.

Linc00662 activated the transcription of ITGA1 through GTF2B in a m⁶A-dependent manner

To elucidate the downstream mechanism of Linc00662 in the malignant progression and

metastasis of PC, we analyzed the subcellular location of Linc00662 using FISH. The result showed that Linc00662 was localized in both the nucleus and cytoplasm of PC cells (**Figure 6A**), indicating that Linc00662 may regulate gene expression. KEGG enrichment analysis was conducted to identify abnormally regulated pathways in differentially expressed mRNAs between METTL3-knockdown cells and control cells. The results showed that focal adhesion was the most-commonly enriched signaling pathway (**Figure 6B**), and three differentially expressed mRNAs were involved in the focal adhesion pathway: integrin alpha-1 (ITGA1), JUN, and CCND2 (**Figure 6C**).

Integrins (ITGs) play a key role in the formation of focal adhesion, which mediates the adhesion of cell to cell and cell to ECM to induce cell growth and metastasis [26]. We examined ITGA1 expression in PC cells and found that the knockdown of METTL3 significantly reduced the expression of ITGA1 at both the RNA and protein levels (**Figure 6D, 6E**). To verify whether Linc00662 m⁶A methylation regulates ITGA1 expression, we knocked down Linc00662 in PC cells and found that the knockdown of Linc00662 down-regulated ITGA1 expression. Conversely, overexpression of Linc00662 Wt exhibited the opposite regulation, but Linc00662 Mut failed (**Figure 6F-H**). Correlation analysis revealed a positive correlation between Linc00662 and ITGA1 expression ($P = 5.5e-06$) (**Figure 6I**). These results indicated that Linc00662 played an important role in the adhesion of PC cells by regulating ITGA1 expression in a m⁶A-dependent manner.

Linc00662 m⁶A promotes PC progression

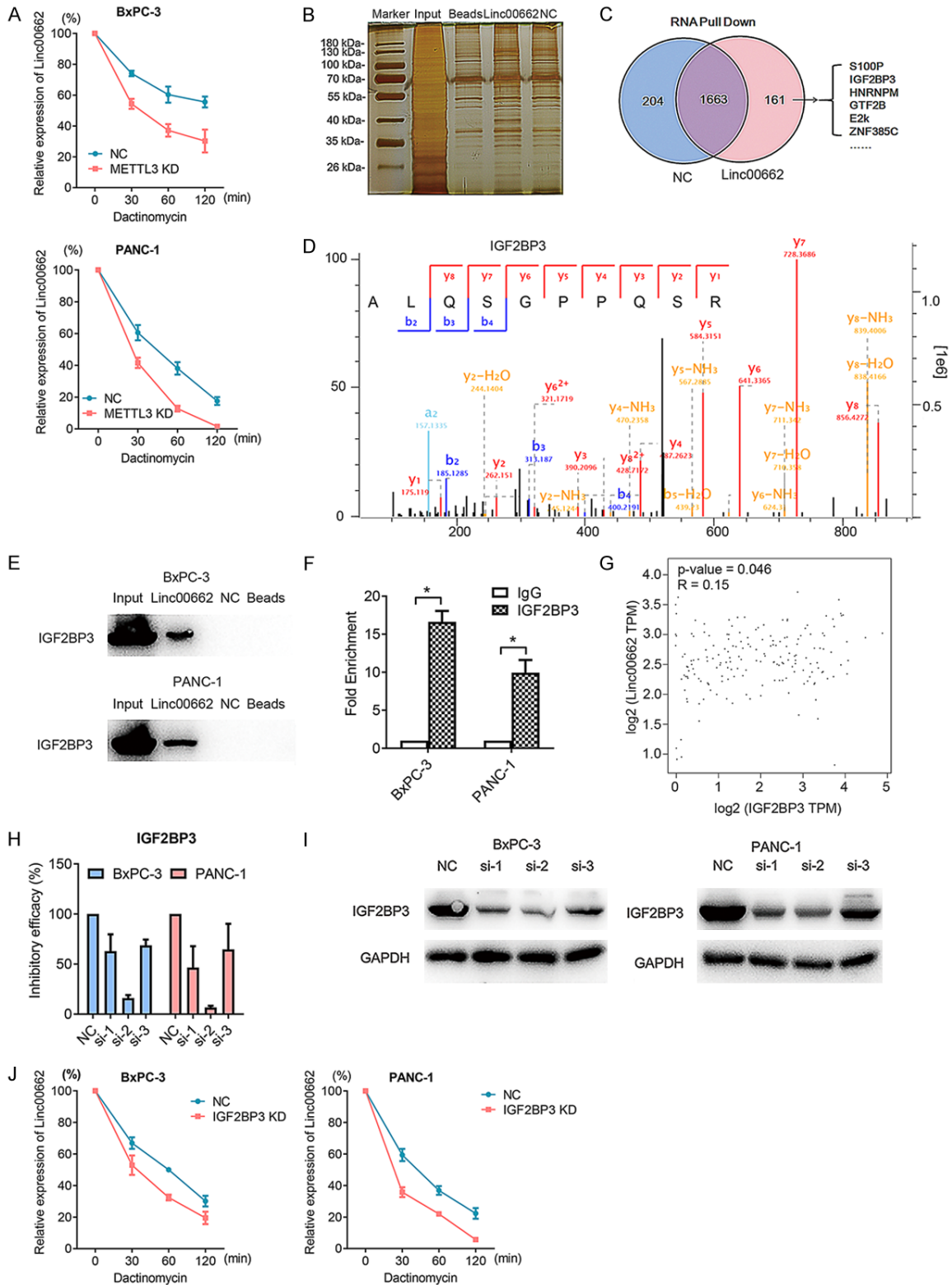
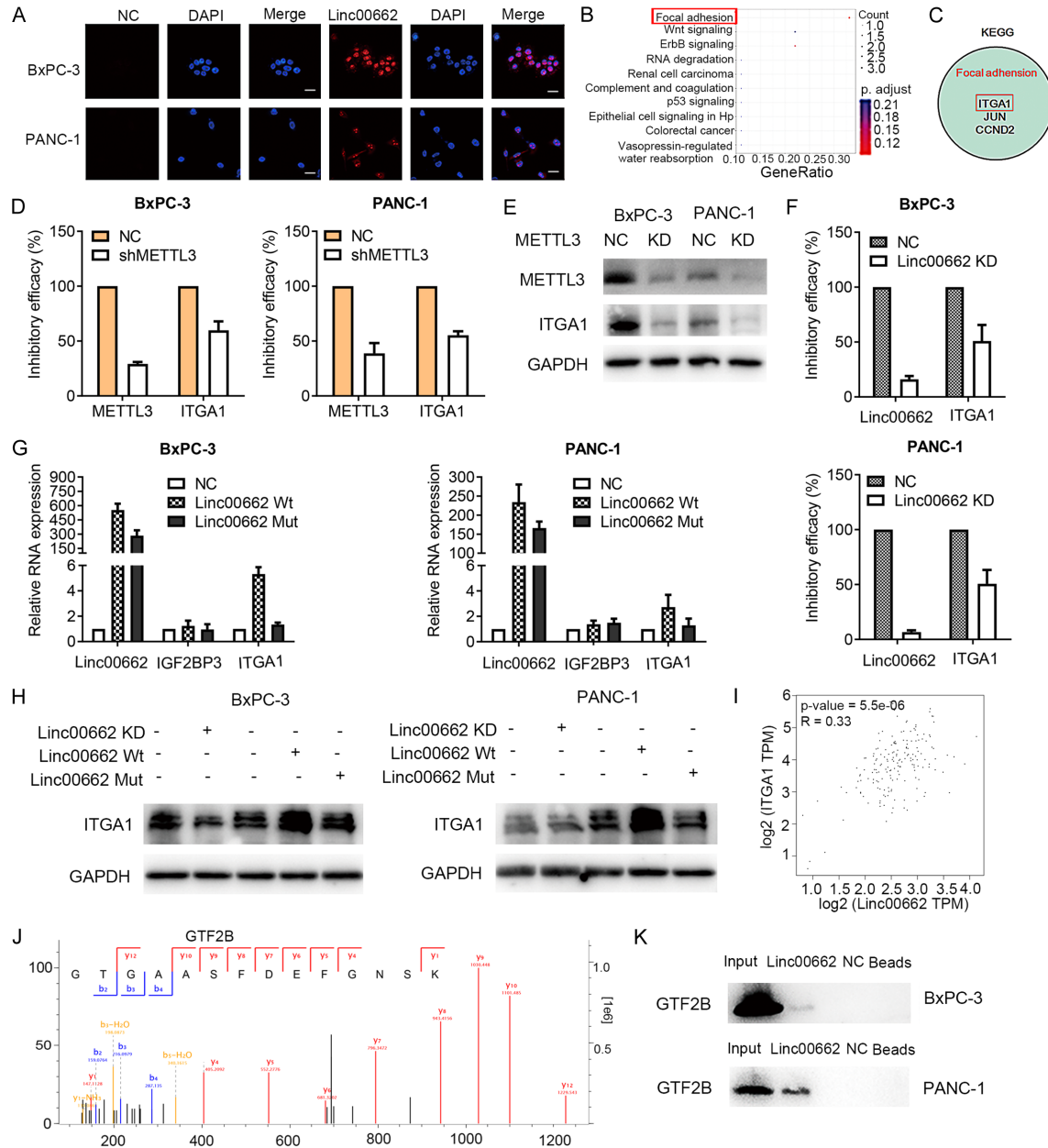


Figure 5. IGF2BP3 regulated the stability of Linc00662 as a m⁶A reader. A. The knockdown of METTL3 in PC cells reduced the half-life of Linc00662 compared to that in control cells. B. The RNA Pull down/MS was conducted to identify the proteins bound to Linc00662. The image of silver staining was displayed to show the proteins pulled down. C. The results of MS showed that IGF2BP3 was the only member of the IGF2BPs bound to Linc00662. D. The secondary structure of IGF2BP3. E. The proteins pulled down with the Linc00662 probe were examined by western

Linc00662 m⁶A promotes PC progression

blotting and the results showed that IGF2BP3 was a component of the complexes. F. The RIP assay confirmed that Linc00662 was enriched in the IGF2BP3 group but not in the IgG group. Bar chart showed the fold enrichment of Linc00662 normalized by IgG in PC cells. *: $P < 0.05$. G. Correlation analysis showed that IGF2BP3 expression was positively related with Linc00662 expression in PC tissues ($P = 0.046$) using the online bioinformatics analysis tool (GEPIA). H. IGF2BP3 was knocked down in PC cells using siRNAs. And IGF2BP3 si-2 showed the highest inhibitory efficacy by qPCR. I. IGF2BP3 was knocked down in PC cells using siRNAs and western blotting confirmed that IGF2BP3 si-2 showed the highest inhibitory efficacy. J. The knockdown of IGF2BP3 in PC cells reduced the half-life of Linc00662 compared to that in control cells. Abbreviations: PC: pancreatic cancer, NC: negative control, Wt: wide type, Mut: 4A-mutated, RIP: RNA immunoprecipitation, qPCR: quantitative polymerase chain reaction, MS: mass spectrometry, m⁶A: N⁶-methyladenosine.



Linc00662 m⁶A promotes PC progression

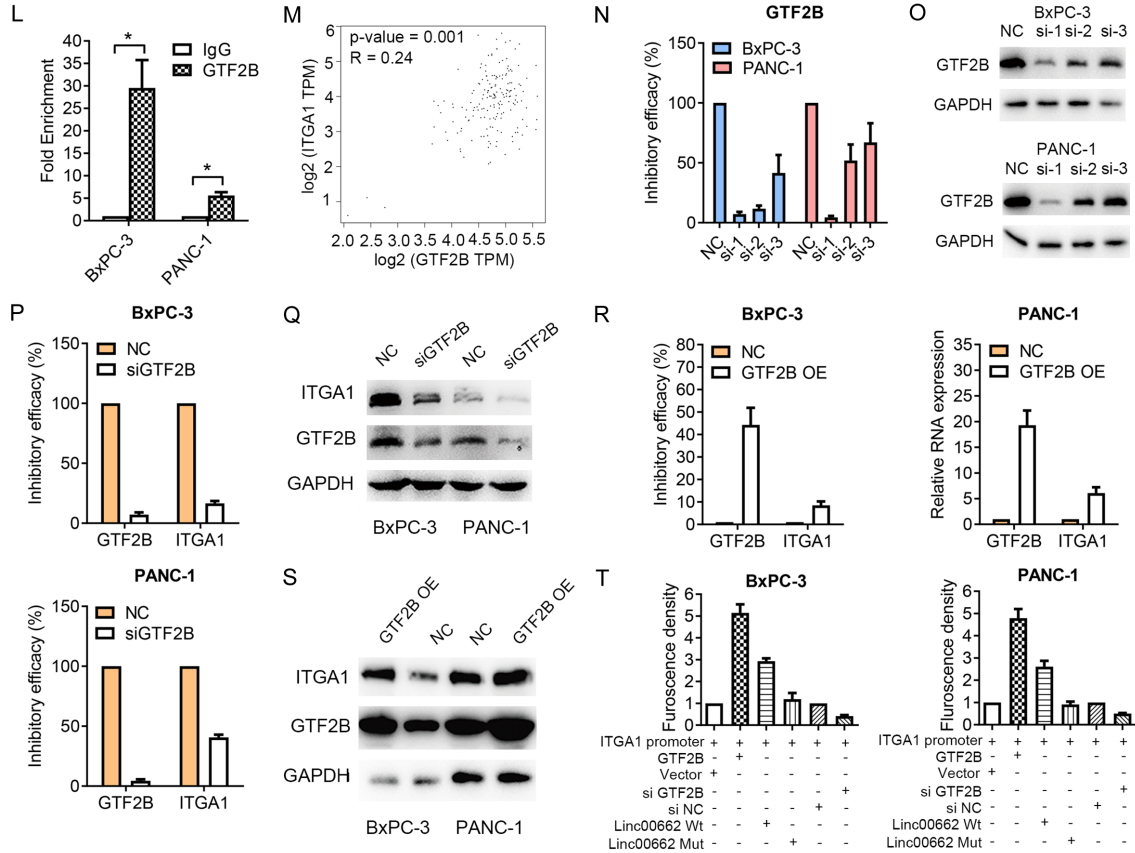


Figure 6. Linc00662 regulated GTF2B-mediated ITGA1 transcription in a m⁶A-dependent manner. A. The subcellular location of Linc00662 was analyzed using FISH. The result showed that Linc00662 was localized in both the nucleus and cytoplasm of PC cells. Scale bar: 20 μ m. B. KEGG enrichment analysis identified focal adhesion as the most commonly enriched signaling pathway associated with METTL3. C. Three differentially expressed mRNAs were involved in the focal adhesion pathway: integrin alpha-1 (ITGA1), JUN, and CCND2. D. The results showed that the knockdown of METTL3 reduced the expression of ITGA1 in PC cells using qPCR. E. The results showed that the knockdown of METTL3 reduced the expression of ITGA1 in PC cells by western blotting. F. The results showed that the knockdown of Linc00662 reduced the expression of ITGA1 in PC cells using qPCR. G. The results showed that the overexpression of Linc00662 Wt increased the expression of ITGA1 in PC cells using qPCR. H. The results showed that the overexpression of Linc00662 Mut failed to affect the expressions of ITGA1 and IGF2BP3 in PC cells using qPCR. I. The results showed that the overexpression of Linc00662 Wt increased the protein expression of ITGA1, but Linc00662 Mut failed and the knockdown of Linc00662 reduced the protein expression of ITGA1 by western blotting. J. Correlation analysis revealed a positive correlation between Linc00662 and ITGA1 expression ($P = 5.5e-06$) using the online bioinformatics analysis tool (GEPIA). K. The secondary structure of GTF2B. L. The proteins pulled down with the Linc00662 probe were examined by western blotting and the results showed that GTF2B was a component of the complexes. M. The RIP assay confirmed that Linc00662 was enriched in the GTF2B group but not in the IgG group. Bar chart showed the fold enrichment of Linc00662 normalized by IgG in PC cells. *: $P < 0.05$. N. Correlation analysis indicated that ITGA1 expression was positively related with GTF2B expression ($P = 0.001$) using the online bioinformatics analysis tool (GEPIA). O. GTF2B was knocked down in PC cells using siRNAs and qPCR examined the inhibitory efficacy. The result indicated that GTF2B si-1 showed the highest inhibitory efficacy. P. GTF2B was knocked down in PC cells using siRNAs and western blotting examined the inhibitory efficacy. The result indicated that GTF2B si-1 showed the highest inhibitory efficacy. Q. The result indicated that the knockdown of GTF2B in PC cells reduced the expression of ITGA1 using qPCR. R. The result indicated that the knockdown of GTF2B in PC cells reduced the expression of ITGA1 by western blotting. S. The result indicated that the overexpression of GTF2B increased the expression of ITGA1 in PC cells using qPCR. T. The result indicated that the overexpression of GTF2B increased the protein expression of ITGA1 in PC cells by western blotting. U. The dual-luciferase reporter assay was conducted to examine the transcriptional role of GTF2B on ITGA1 and the role of m⁶A modification in Linc00662 on ITGA1 transcription. The results indicated that GTF2B overexpression increased fluorescence intensity, and knockdown of GTF2B decreased fluorescence intensity. In addition, the overexpression of Linc00662 Wt increased the fluorescence intensity, but Linc00662 Mut failed. Abbreviations: PC: pancreatic cancer, NC: negative control, Wt: wide type, Mut: 4A-mutated, RIP: RNA immunoprecipitation, qPCR: quantitative polymerase chain reaction, GTF2B: general transcription factor II-B, ITGA1: integrin alpha-1, m⁶A: N6-methyladenosine.

However, an RNA pull-down assay failed to demonstrate a direct interaction between Linc00662 and ITGA1, suggesting that Linc00662 may regulate ITGA1 expression by binding to transcription factors. To further investigate the mechanism by which Linc00662 regulates ITGA1 expression, we analyzed the binding proteins specific to Linc00662 using RNA pull-down and identified several transcription factors. GTF2B attracted our interest (**Figure 6J**), because it has been reported that GTF2B regulated ITGA2 transcription in colon cancer [28]. Western blotting confirmed that GTF2B bound to Linc00662 (**Figure 6K**), and RIP assay verified that Linc00662 was enriched in the GTF2B group but not in the IgG group (**Figure 6L**). In addition, correlation analysis indicated that ITGA1 expression was positively related to GTF2B expression ($P = 0.001$) (**Figure 6M**).

We examined the effect of GTF2B on ITGA1 expression. GTF2B was knocked down in PC cells using siRNA. qPCR and western blotting indicated that GTF2B si-1 showed the highest inhibitory efficacy (**Figure 6N, 6O**) and was used for further study. The results showed that the knockdown of GTF2B in PC cells reduced the expression of ITGA1 at both the RNA and protein levels (**Figure 6P, 6Q**). However, the overexpression of GTF2B exhibited the opposite effects in PC cells (**Figure 6R, 6S**). These results indicate that GTF2B may play a transcriptional role in ITGA1. To verify this, we conducted a dual-luciferase reporter assay and found that GTF2B overexpression increased fluorescence intensity, and knockdown of GTF2B decreased fluorescence intensity, indicating that GTF2B promoted ITGA1 expression by binding to its promoter (**Figure 6T**). Furthermore, the overexpression of Linc00662 Wt increased the fluorescence intensity, but Linc00662 Mut failed (**Figure 6T**), indicating that m⁶A methylation is required for Linc00662 to promote GTF2B-mediated ITGA1 transcription.

Linc00662 initiated focal adhesion through ITGA1/FAK pathway to promote the malignant progression and metastasis of PC

Next, we verified whether Linc00662 promoted PC malignant progression and metastasis by activating ITGA1-mediated focal adhesions.

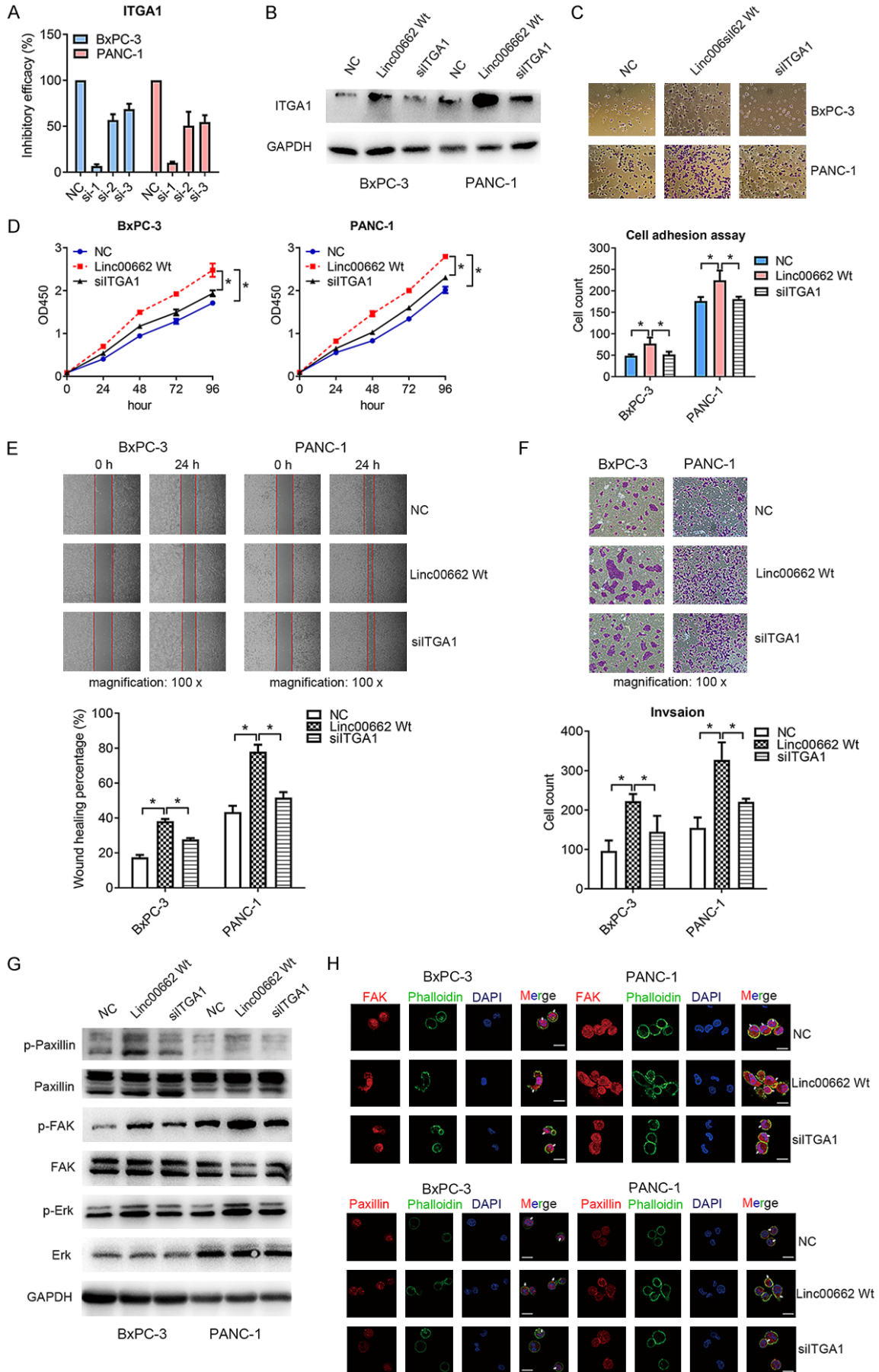
Rescue experiments were conducted by down-regulating ITGA1 in Linc00662-overexpressing PC cells (**Figure 7A, 7B**). As a result, overexpression of Linc00662 in PC cells not only enhanced the ability of cells to adhere to collagen (**Figure 7C**) and promoted the proliferative, migratory, and invasive capacities of PC cells (**Figure 7D-F**), but also dramatically upregulated the levels of p-FAK, p-Paxillin and p-Erk, which could be reversed by the knockdown of ITGA1 (**Figure 7G**). Furthermore, the effects of Linc00662 on the morphology and location of focal adhesions in PC cells were examined by staining the cells with focal adhesion markers (FAK and Paxillin) and observation by confocal microscopy. As shown in **Figure 7H**, compared with the control cells, more obvious pseudopods were observed in Linc00662-overexpression cells, and more FAK and Paxillin were localized on the leading edge of the plasma membrane, which could be reversed by the knockdown of ITGA1. These results strongly suggest that Linc00662 promotes the proliferation, invasion, and migration of PC cells by facilitating the formation of focal contacts through the ITGA1/FAK pathway.

Y15 is a potent and specific inhibitor of FAK, which triggered our interest in examining its potential as a therapeutic agent against Linc00662-overexpressing PC cells. As shown in **Figure 8A**, the suitable concentrations of Y15 were 2 μ M and 5 μ M in Linc00662-overexpressing BxPC-3 cells and Linc00662-overexpressing PANC-1 cells, respectively, which inhibited FAK autophosphorylation activity without effect on FAK expression. These screened concentrations of Y15 were used in further studies. The results showed that Y15 treatment not only dramatically repressed the activity of p-FAK, p-Paxillin and p-Erk in PC cells (**Figure 8B**), but also significantly reversed the increased proliferative, migratory, and invasive capacities of Linc00662-overexpressing PC cells (**Figure 8C-E**). *In vivo*, Y15 inhibited subcutaneous tumor growth in mice bearing Linc00662-overexpressed PC cells (**Figure 8F-H**).

Discussion

To the best of our knowledge, this is the first study confirming that Linc00662 is enriched with m⁶A methylation and closely associated

Linc00662 m⁶A promotes PC progression



Linc00662 m⁶A promotes PC progression

Figure 7. Linc00662 promoted the malignant progression by regulating ITGA1 transcription in PC. A. ITGA1 was knocked down in PC cells using siRNAs and qPCR was used to examine the inhibitory efficacy. The result indicated that ITGA1 si-1 showed the highest inhibitory efficacy. B. Western blotting revealed that the overexpression of Linc00662 Wt increased the expression of ITGA1, which could be reversed by the knockdown of ITGA1 using si-ITGA1. C. The cell adhesion assay revealed that the overexpression of Linc00662 in PC cells enhanced the ability of cells to adhere to collagen. Representative micrographs were displayed and the bar charts showed the differences of cell numbers adhere to collagen among Linc00662 Wt, siITGA1, and control cells. *: $P < 0.05$, magnification: 100 ×. D. The CCK8 assay showed that the cell proliferative capacity was significantly increased in Linc00662 Wt cells, which could be reversed by the knockdown of ITGA1 using siITGA1. E. The wound healing assay indicated that the overexpression of Linc00662 Wt significantly increased cell migratory capacity, which could be reversed by the knockdown of ITGA1 using siITGA1. Representative micrographs were displayed and the bar charts showed the differences of migratory area among Linc00662 Wt, siITGA1, and control cells. *: $P < 0.05$, magnification: 100 ×. F. The transwell assay revealed that the overexpression of Linc00662 Wt significantly increased cell invasive capacity, which could be reversed by the knockdown of ITGA1 using siITGA1. Representative micrographs were displayed and the bar charts showed the differences of invaded cell numbers among Linc00662 Wt, siITGA1, and control cells. *: $P < 0.05$, magnification: 100 ×. G. Western blotting showed that the overexpression of Linc00662 Wt dramatically upregulated the levels of p-FAK, p-Paxillin and p-Erk, which could be reversed by the knockdown of ITGA1. H. The immunofluorescence assay revealed that the overexpression of Linc00662 Wt caused morphology change with more obvious pseudopods, and more FAK and Paxillin localized on the leading edge of the plasma membrane, which could be reversed by the knockdown of ITGA1. White arrows indicated the location of focal adhesion markers (FAK and Paxillin). Scale bar: 30 μm. Abbreviations: PC: pancreatic cancer, NC: negative control, Wt: wide type, Mut: 4A-mutated, qPCR: quantitative polymerase chain reaction, CCK8: cell counting kit-8, GTF2B: general transcription factor II-B, ITGA1: integrin alpha-1.

with disease progression and poor prognosis in PC. Moreover, we found that Linc00662 promoted PC cell proliferation, migration, and invasion *in vitro* and promoted tumor growth and metastasis *in vivo* in a m⁶A-dependent manner. Interestingly, further experiments showed that m⁶A-enriched Linc00662 recruited GTF2B to regulate the transcription of ITGA1, thereby activating the formation of focal adhesions via the ITGA1-FAK-Erk pathway.

In this study, we first confirmed that METTL3 upregulation promotes malignant behavior in PC cells, which is consistent with previous reports [17, 19]. Furthermore, we analyzed the relationship between METTL3 expression and the clinical prognosis of patients with PC enrolled at our hospital. Although there was a negative relationship between METTL3 expression and PFS, a novel lncRNA 00662 (Linc00662) was identified with enriched m⁶A methylation was identified. Although previous studies have identified Linc00662 played oncogenic roles in melanoma and hepatocellular carcinoma [29, 30], our study is the first to prove that Linc00662 played oncogenic roles in PC in a m⁶A-dependent manner. m⁶A methylation is involved in diverse regulatory processes, including RNA stability, decay, nuclear retention, and translation [31], and participates in a variety of processes, such as tumor proliferation, invasion, epithelial-mesenchymal transition (EMT), and metastasis [32-34]. It has

been reported that m⁶A in MALAT1 is associated with HNRNPC and affects target gene expression [35], while m⁶A in Xist binds to YTHDC1 to mediate transcript silencing [36]. This study verified that m⁶A in Linc00662 is bound to IGF2BP3 to maintain its stability and is required for its oncogenic properties in PC. These findings expand our understanding of the functions and upstream regulatory mechanisms of m⁶A methylation in lncRNAs.

Integrins (ITGs) are a family of heterodimeric cell surface adhesion molecules [37] that transmit intracellular signals as primary transmembrane receptors when bound to their respective extracellular matrix (ECM) proteins, thereby potentially mediating cell adhesion, proliferation, migration, and invasion [38]. It has been reported that ITGA1 was associated with invasive or metastatic phenotypes in hepatocellular and prostate cancers [39, 40]. A recent study reported that ITGA1 is frequently upregulated in PC and mediates TGFβ/collagen-induced EMT and gemcitabine resistance in PC cells, which is associated with poor patient prognosis [41]. In this study, we found that Linc00662 promoted cell adhesion, proliferation, migration, and invasion through ITGA1 activation.

ITGA1 initiates the formation of focal adhesions, which contain an array of proteins such as focal adhesion kinase (FAK), steroid recep-

Linc00662 m⁶A promotes PC progression

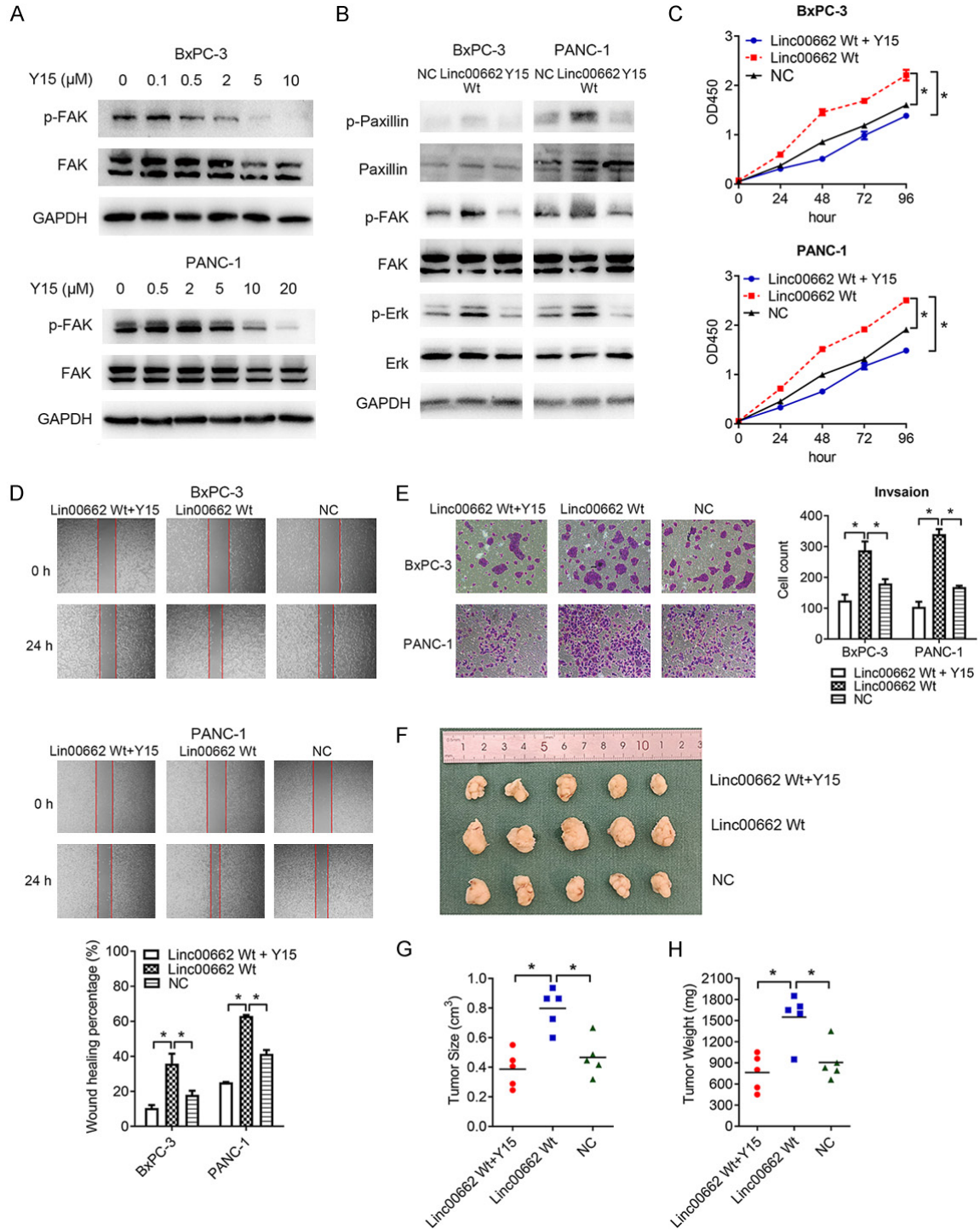


Figure 8. The FAK inhibitor-Y15 repressed the malignant progression of PC. A. Linc00662-overexpressing PC cells were treated with Y15 at different concentrations to identify the suitable concentrations. The results of western blotting showed that 2 μM and 5 μM of Y15 were the suitable concentrations in BxPC-3 cells and PANC-1 cells, respectively, which inhibited FAK autophosphorylation activity without effect on FAK expression. B. Western blotting showed that Y15 treatment dramatically repressed the levels of p-FAK, p-Paxillin, and p-Erk in PC cells. C. The CCK8 assay showed that Y15 treatment significantly reversed the increased proliferative capacity of Linc00662-overexpressing PC cells. D. The wound healing assay indicated that Y15 treatment significantly reversed the increased migratory capacity of Linc00662-overexpressing PC cells, magnification: 100 ×. E. The transwell assay indicated that Y15 treatment significantly reversed the increased invasive capacity of Linc00662-overexpressing PC cells,

Linc00662 m⁶A promotes PC progression

magnification: 100 ×. F. A mouse xenograft model was used to evaluate the effect of Y15 on cell growth *in vivo*. Images of transplanted subcutaneous tumors were displayed. G. Y15 treatment dramatically repressed tumor volume in mice bearing Linc00662-overexpressed PC cells. *: $P < 0.05$. H. Y15 treatment dramatically repressed subcutaneous tumor weight in mice bearing Linc00662-overexpressed PC cells. *: $P < 0.05$. Abbreviations: PC: pancreatic cancer, CCK8: cell counting kit-8.

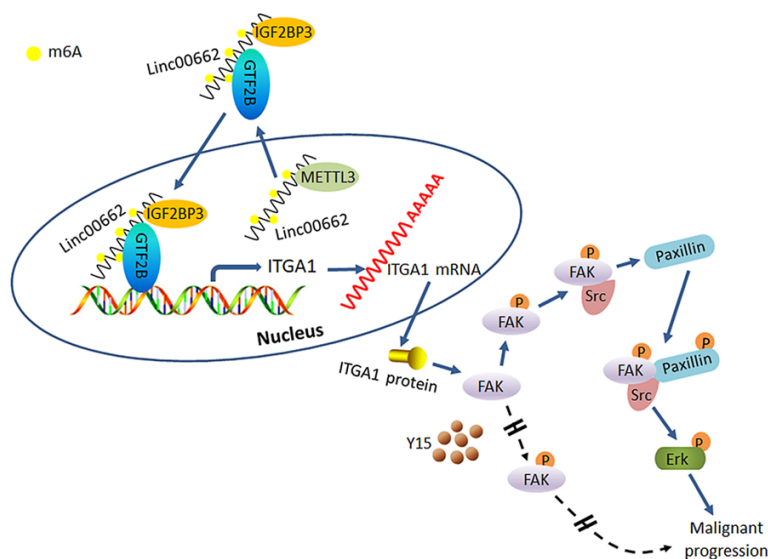


Figure 9. Schematic model on the role of Linc00662 in regulating PC malignant progression through the GTF2B-ITGA1-FAK pathway. This study proposes a novel regulatory mechanism of Linc00662 in oncogene activation in PC. Linc00662 activates the transcription of ITGA1 by recruiting GTF2B in a m6A-dependent manner and promotes PC cell proliferation, invasion, and migration, which partly relies on the activation of focal adhesions through the ITGA1-FAK-Erk pathway. And Y15 treatment inhibits autophosphorylation of FAK and obviously represses tumor progression of Linc00662-overexpressing PC cells. Abbreviations: PC: pancreatic cancer, GTF2B: general transcription factor II-B, ITGA1: integrin alpha-1, m6A: N6-methyladenosine.

tor coactivator (Src) and paxillin [42, 43]. FAK is a typical protein that is highly autophosphorylated in response to integrin activation. FAK can regulate cytoskeleton dynamics and cell movement by affecting actin polymerization and focal adhesion inversion and has diverse cellular functions, including cell proliferation, adhesion, and migration [44]. Paxillin is a typical focal adhesion adaptor protein that recruits key components of its signal transduction machinery to specific subcellular locations, including FAK and Src. Phosphorylated FAK in association with Src phosphorylates paxillin, which is associated with the coordinated formation of focal adhesions [45]. Our study verified that Linc00662 activated focal adhesion, as evidenced by increased levels of p-FAK and p-Paxillin, more obvious pseudopodia, and more FAK and Paxillin on the leading edge at

the periphery in Linc00662-overexpressing cells.

Phosphorylated FAK and Src form complexes that activate or inhibit multiple downstream signaling pathways, including PI3K/Akt, P53, Erk. The Src/FAK-Erk signaling pathway plays an important role in tumorigenesis and metastasis of various cancers, including NSCLC [46-48]. For example, PIG3 enhances cell migration and invasion by promoting the Src/FAK-Erk pathway in lung adenocarcinomas [49]. Matrilin inhibits migration and invasion of NSCLC cells through repressing the Src/FAK-Erk- β -catenin signaling [50]. Our study identified Linc00662 promoted cell proliferation, migration, and invasion by activating ITGA1-Src/FAK-Erk signaling, as evidenced by the increased levels of p-FAK, p-Paxillin, and p-Erk in

Linc00662-overexpressing cells, which could be reversed by the knockdown of ITGA1.

Targeting ITGA1 or its downstream molecules is a potential strategy for PC management. Several approaches have been used to target FAK activity in cancer cells. Initial trials involved FAK knockdown using siRNA, antisense oligonucleotides, and adenoviral dominant-negative FAK-CD. These methods induce a significant down-regulation of FAK, inhibit cancer cell proliferation, increase apoptosis, and decrease tumorigenicity [51-53]. However, these approaches have limitations in clinical research due to their *in vivo* toxicity. This has led to the development of small molecule inhibitors of FAK, which include inhibitors that target enzymatic kinase dependent or independent functions of FAK [54-56]. In this study, Y15, an en-

zymatic kinase dependent FAK inhibitor that inhibits its autophosphorylation activity and its downstream targets, repressed tumor progression in Linc00662-overexpressing PC cells *in vitro* and *in vivo*. It has been reported that a combination of FAK inhibitors and inhibitors of other signaling molecules is more effective than a single drug alone [57]. Several studies have been conducted, ranging from bench work to clinical trials. The combination of the FAK inhibitor Y15 and Src inhibitor PP2 significantly decreased the viability of colon cancer cells [58]. The combination of the FAK inhibitor Y15 with gemcitabine was more effective in suppressing pancreatic cancer tumor growth in a mouse xenograft model than a single drug alone [56]. Currently, FAK inhibitors in combination with other inhibitors are under phase I/II safety and pharmacokinetics evaluation for the treatment of advanced solid cancers; however, the true potential of single or combinatorial therapies remains unclear. These results suggest that FAK inhibitors are promising therapeutic agents for PC with a high expression of Linc00662.

This study had some limitations. First, the sample size of PC tissues collected from our hospital was small, and the overall survival was not currently available owing to time limitation. Second, the m⁶A motifs of Linc00662 that interacted with IGF2BP3 were not explored. Third, a tail vein metastasis model was used to study the general metastatic features of tumor cells *in vivo*. For further in-depth studies, a liver-metastatic model should be used, because pancreatic cancer usually metastasizes to the liver. Lastly, the METTL3-METTL14 heterodimeric complex generates m⁶A on mRNA, where METTL3 contributes the catalytic residues, while METTL14 provides structural supports for METTL3; however the involvement of METTL14 in the process deserves further exploration.

Conclusions

This study proposes a novel regulatory mechanism for Linc00662 in oncogene activation in PC. Linc00662 activates the transcription of ITGA1 by recruiting GTF2B in a m⁶A-dependent manner and promotes PC cell proliferation, invasion, and migration, which partly relies on the activation of focal adhesions through the ITGA1-FAK-Erk pathway. These results indicated that Linc00662 and downstream molecules

could be potential molecular targets for PC therapy (Figure 9).

Acknowledgements

We are indebted to all the authors and our colleagues for the fruitful suggestions and discussions. This work was supported by Jiangsu Natural Science Foundation Project (No. BK20191142), High-level talent training project of Wuxi Taihu Talent Plan (No. BJ2020055), Science and Technology Development Plan Project of Wuxi (No. N20202011), Scientific Research Project of Jiangsu Provincial Health Commission (No. Z2018022), Major scientific research project of Wuxi Municipal Health Commission (No. Z201805), Research team construction funding project of Jiangnan University School of Medicine (No. 2860102-42190110), Translational Medicine Research Project of Wuxi Municipal Health Commission (No. ZM002), Special Funding of Science and Education Enhancing Health of Wuxi (No. QNRC015), Young Researcher Grants Program of Wuxi Health and Family Planning Commission (No. Q201621).

The signed informed consents were obtained from all the patients.

Disclosure of conflict of interest

None.

Abbreviations

m⁶A, N⁶-methyladenosine; LncRNA, Long non-coding RNA; PC, Pancreatic cancer; RIP, RNA immunoprecipitation; MeRIP, Methylated RNA immunoprecipitation; HPNE, human pancreatic ductal epithelial cell line; qPCR, quantitative polymerase chain reaction; shRNA, small hairpin RNA; PFA, paraformaldehyde; CCK8, Cell counting kit-8; H&E, hematoxylin and eosin; FC, fold change; GEO, Gene Expression Omnibus; FISH, Fluorescence in situ hybridization; NC, negative control; KD, knock down; Wt, wide type; Mut, 4A-mutated; MS, mass spectrometry; GTF2B, general transcription factor IIB; ITGA1, integrin alpha-1.

Address correspondence to: Hao Hu and Youzhao He, Hepatobiliary and Pancreatic Surgery, Affiliated Hospital of Jiangnan University, 1000 Hefeng Rd, Binhu District, Wuxi 214122, Jiangsu, China. E-mail: haohu@ntu.edu.cn (HH); wxgdyzx@163.com (YZH)

References

- [1] Hidalgo M. Pancreatic cancer. *N Engl J Med* 2010; 362: 1605-1617.
- [2] Garrido-Laguna I and Hidalgo M. Pancreatic cancer: from state-of-the-art treatments to promising novel therapies. *Nat Rev Clin Oncol* 2015; 12: 319-334.
- [3] Siegel RL, Miller KD, Fuchs HE and Jemal A. Cancer statistics, 2022. *CA Cancer J Clin* 2022; 72: 7-33.
- [4] Chiorean EG and Covelev AL. Pancreatic cancer: optimizing treatment options, new, and emerging targeted therapies. *Drug Des Devel Ther* 2015; 9: 3529-3545.
- [5] Wang X, Feng J, Xue Y, Guan Z, Zhang D, Liu Z, Gong Z, Wang Q, Huang J, Tang C, Zou T and Yin P. Corrigendum: structural basis of N(6)-adenosine methylation by the METTL3-METTL14 complex. *Nature* 2017; 542: 260.
- [6] Ping XL, Sun BF, Wang L, Xiao W, Yang X, Wang WJ, Adhikari S, Shi Y, Lv Y, Chen YS, Zhao X, Li A, Yang Y, Dahal U, Lou XM, Liu X, Huang J, Yuan WP, Zhu XF, Cheng T, Zhao YL, Wang X, Rendtlew Danielsen JM, Liu F and Yang YG. Mammalian WTAP is a regulatory subunit of the RNA N6-methyladenosine methyltransferase. *Cell Res* 2014; 24: 177-189.
- [7] Jia G, Fu Y, Zhao X, Dai Q, Zheng G, Yang Y, Yi C, Lindahl T, Pan T, Yang YG and He C. N6-methyladenosine in nuclear RNA is a major substrate of the obesity-associated FTO. *Nat Chem Biol* 2011; 7: 885-887.
- [8] Tang C, Klukovich R, Peng H, Wang Z, Yu T, Zhang Y, Zheng H, Klungland A and Yan W. ALKBH5-dependent m6A demethylation controls splicing and stability of long 3'-UTR mRNAs in male germ cells. *Proc Natl Acad Sci U S A* 2018; 115: E325-E333.
- [9] Du H, Zhao Y, He J, Zhang Y, Xi H, Liu M, Ma J and Wu L. YTHDF2 destabilizes m(6)A-containing RNA through direct recruitment of the CCR4-NOT deadenylase complex. *Nat Commun* 2016; 7: 12626.
- [10] Zhou J, Wan J, Gao X, Zhang X, Jaffrey SR and Qian SB. Dynamic m(6)A mRNA methylation directs translational control of heat shock response. *Nature* 2015; 526: 591-594.
- [11] Bokar JA, Shambaugh ME, Polayes D, Matera AG and Rottman FM. Purification and cDNA cloning of the AdoMet-binding subunit of the human mRNA (N6-adenosine)-methyltransferase. *RNA* 1997; 3: 1233-1247.
- [12] Bokar JA, Rath-Shambaugh ME, Ludwiczak R, Narayan P and Rottman F. Characterization and partial purification of mRNA N6-adenosine methyltransferase from HeLa cell nuclei. Internal mRNA methylation requires a multisubunit complex. *J Biol Chem* 1994; 269: 17697-17704.
- [13] Lin S, Choe J, Du P, Triboulet R and Gregory RI. The m(6)A methyltransferase METTL3 promotes translation in human cancer cells. *Mol Cell* 2016; 62: 335-345.
- [14] Sorci M, Ianniello Z, Cruciani S, Larivera S, Ginistrelli LC, Capuano E, Marchioni M, Fazi F and Fatica A. METTL3 regulates WTAP protein homeostasis. *Cell Death Dis* 2018; 9: 796.
- [15] Li X, Tang J, Huang W, Wang F, Li P, Qin C, Qin Z, Zou Q, Wei J, Hua L, Yang H and Wang Z. The M6A methyltransferase METTL3: acting as a tumor suppressor in renal cell carcinoma. *Oncotarget* 2017; 8: 96103-96116.
- [16] Dai D, Wang H, Zhu L, Jin H and Wang X. N6-methyladenosine links RNA metabolism to cancer progression. *Cell Death Dis* 2018; 9: 124.
- [17] Wang L, Zhang S, Li H, Xu Y, Wu Q, Shen J, Li T and Xu Y. Quantification of m6A RNA methylation modulators pattern was a potential biomarker for prognosis and associated with tumor immune microenvironment of pancreatic adenocarcinoma. *BMC Cancer* 2021; 21: 876.
- [18] Xu F, Zhang Z, Yuan M, Zhao Y, Zhou Y, Pei H and Bai L. M6A regulatory genes play an important role in the prognosis, progression and immune microenvironment of pancreatic adenocarcinoma. *Cancer Invest* 2021; 39: 39-54.
- [19] Xia T, Wu X, Cao M, Zhang P, Shi G, Zhang J, Lu Z, Wu P, Cai B, Miao Y and Jiang K. The RNA m6A methyltransferase METTL3 promotes pancreatic cancer cell proliferation and invasion. *Pathol Res Pract* 2019; 215: 152666.
- [20] Taketo K, Konno M, Asai A, Koseki J, Toratani M, Satoh T, Doki Y, Mori M, Ishii H and Ogawa K. The epitranscriptome m6A writer METTL3 promotes chemo- and radioresistance in pancreatic cancer cells. *Int J Oncol* 2018; 52: 621-629.
- [21] Wang X, Lu Z, Gomez A, Hon GC, Yue Y, Han D, Fu Y, Parisien M, Dai Q, Jia G, Ren B, Pan T and He C. N6-methyladenosine-dependent regulation of messenger RNA stability. *Nature* 2014; 505: 117-120.
- [22] Wang X, Zhao BS, Roundtree IA, Lu Z, Han D, Ma H, Weng X, Chen K, Shi H and He C. N(6)-methyladenosine modulates messenger RNA translation efficiency. *Cell* 2015; 161: 1388-1399.
- [23] Bao H and Su H. Long noncoding RNAs act as novel biomarkers for hepatocellular carcinoma: progress and prospects. *Biomed Res Int* 2017; 2017: 6049480.
- [24] Klingenberg M, Matsuda A, Diederichs S and Patel T. Non-coding RNA in hepatocellular carcinoma: mechanisms, biomarkers and therapeutic targets. *J Hepatol* 2017; 67: 603-618.
- [25] Zuo X, Chen Z, Gao W, Zhang Y, Wang J, Wang J, Cao M, Cai J, Wu J and Wang X. M6A-mediated upregulation of LINC00958 increases lipo-

- genesis and acts as a nanotherapeutic target in hepatocellular carcinoma. *J Hematol Oncol* 2020; 13: 5.
- [26] Liu H, Xu Y, Yao B, Sui T, Lai L and Li Z. A novel N6-methyladenosine (m6A)-dependent fate decision for the lncRNA THOR. *Cell Death Dis* 2020; 11: 613.
- [27] Wen S, Wei Y, Zen C, Xiong W, Niu Y and Zhao Y. Long non-coding RNA NEAT1 promotes bone metastasis of prostate cancer through N6-methyladenosine. *Mol Cancer* 2020; 19: 171.
- [28] Ruan Z, Deng H, Liang M, Xu Z, Lai M, Ren H, Deng X and Su X. Overexpression of long non-coding RNA00355 enhances proliferation, chemotaxis, and metastasis in colon cancer via promoting GTF2B-mediated ITGA2. *Transl Oncol* 2021; 14: 100947.
- [29] Guo T, Gong C, Wu P, Battaglia-Hsu SF, Feng J, Liu P, Wang H, Guo D, Yao Y, Chen B, Xiao Y, Liu Z and Li Z. LINC00662 promotes hepatocellular carcinoma progression via altering genomic methylation profiles. *Cell Death Differ* 2020; 27: 2191-2205.
- [30] Xia XQ, Lu WL, Ye YY and Chen J. LINC00662 promotes cell proliferation, migration and invasion of melanoma by sponging miR-890 to up-regulate ELK3. *Eur Rev Med Pharmacol Sci* 2020; 24: 8429-8438.
- [31] Zheng G, Dahl JA, Niu Y, Fedorcsak P, Huang CM, Li CJ, Vagbo CB, Shi Y, Wang WL, Song SH, Lu Z, Bosmans RP, Dai Q, Hao YJ, Yang X, Zhao WM, Tong WM, Wang XJ, Bogdan F, Furu K, Fu Y, Jia G, Zhao X, Liu J, Krokan HE, Klungland A, Yang YG and He C. ALKBH5 is a mammalian RNA demethylase that impacts RNA metabolism and mouse fertility. *Mol Cell* 2013; 49: 18-29.
- [32] Dominissini D, Moshitch-Moshkovitz S, Schwartz S, Salmon-Divon M, Ungar L, Osenberg S, Cesarkas K, Jacob-Hirsch J, Amariglio N, Kupiec M, Sorek R and Rechavi G. Topology of the human and mouse m6A RNA methylomes revealed by m6A-seq. *Nature* 2012; 485: 201-206.
- [33] Meyer KD, Saletore Y, Zumbo P, Elemento O, Mason CE and Jaffrey SR. Comprehensive analysis of mRNA methylation reveals enrichment in 3'UTRs and near stop codons. *Cell* 2012; 149: 1635-1646.
- [34] Fu Y, Dominissini D, Rechavi G and He C. Gene expression regulation mediated through reversible m(6)A RNA methylation. *Nat Rev Genet* 2014; 15: 293-306.
- [35] Liu N, Dai Q, Zheng G, He C, Parisien M and Pan T. N(6)-methyladenosine-dependent RNA structural switches regulate RNA-protein interactions. *Nature* 2015; 518: 560-564.
- [36] Patil DP, Chen CK, Pickering BF, Chow A, Jackson C, Guttman M and Jaffrey SR. m(6)A RNA methylation promotes XIST-mediated transcriptional repression. *Nature* 2016; 537: 369-373.
- [37] De Franceschi N, Arjonen A, Elkhatib N, Denessiouk K, Wrobel AG, Wilson TA, Pouwels J, Montagnac G, Owen DJ and Ivaska J. Selective integrin endocytosis is driven by interactions between the integrin alpha-chain and AP2. *Nat Struct Mol Biol* 2016; 23: 172-179.
- [38] Gong H, Shen B, Flevaris P, Chow C, Lam SC, Voyno-Yasenetskaya TA, Kozasa T and Du X. G protein subunit Galpha13 binds to integrin alpha5beta3 and mediates integrin "outside-in" signaling. *Science* 2010; 327: 340-343.
- [39] Liu X, Tian H, Li H, Ge C, Zhao F, Yao M and Li J. Derivate isocorydine (d-ICD) suppresses migration and invasion of hepatocellular carcinoma cell by downregulating ITGA1 expression. *Int J Mol Sci* 2017; 18: 514.
- [40] Rosenberg EE, Prudnikova TY, Zabarovsky ER, Kashuba VI and Grigorieva EV. D-glucuronyl C5-epimerase cell type specifically affects angiogenesis pathway in different prostate cancer cells. *Tumour Biol* 2014; 35: 3237-3245.
- [41] Gharibi A, La Kim S, Molnar J, Brambilla D, Adamian Y, Hoover M, Hong J, Lin J, Wolfenden L and Kelber JA. ITGA1 is a pre-malignant biomarker that promotes therapy resistance and metastatic potential in pancreatic cancer. *Sci Rep* 2017; 7: 10060.
- [42] Duxbury MS, Ito H, Zinner MJ, Ashley SW and Whang EE. Focal adhesion kinase gene silencing promotes anoikis and suppresses metastasis of human pancreatic adenocarcinoma cells. *Surgery* 2004; 135: 555-562.
- [43] Liu W, Bloom DA, Cance WG, Kurenova EV, Golubovskaya VM and Hochwald SN. FAK and IGF-IR interact to provide survival signals in human pancreatic adenocarcinoma cells. *Carcinogenesis* 2008; 29: 1096-1107.
- [44] Fife CM, McCarroll JA and Kavallaris M. Movers and shakers: cell cytoskeleton in cancer metastasis. *Br J Pharmacol* 2014; 171: 5507-5523.
- [45] Kanteti R, Batra SK, Lennon FE and Salgia R. FAK and paxillin, two potential targets in pancreatic cancer. *Oncotarget* 2016; 7: 31586-31601.
- [46] Roy-Luzarraga M and Hodivala-Dilke K. Molecular pathways: endothelial cell FAK-A target for cancer treatment. *Clin Cancer Res* 2016; 22: 3718-3724.
- [47] Patel A, Sabbineni H, Clarke A and Somanath PR. Novel roles of Src in cancer cell epithelial-to-mesenchymal transition, vascular permeability, microinvasion and metastasis. *Life Sci* 2016; 157: 52-61.
- [48] Kohno M and Pouyssegur J. Targeting the ERK signaling pathway in cancer therapy. *Ann Med* 2006; 38: 200-211.

Linc00662 m⁶A promotes PC progression

- [49] Gu MM, Gao D, Yao PA, Yu L, Yang XD, Xing CG, Zhou J, Shang ZF and Li M. p53-inducible gene 3 promotes cell migration and invasion by activating the FAK/Src pathway in lung adenocarcinoma. *Cancer Sci* 2018; 109: 3783-3793.
- [50] Ku MJ, Kim JH, Lee J, Cho JY, Chun T and Lee SY. Maclurin suppresses migration and invasion of human non-small-cell lung cancer cells via anti-oxidative activity and inhibition of the Src/FAK-ERK-beta-catenin pathway. *Mol Cell Biochem* 2015; 402: 243-252.
- [51] Xu LH, Yang X, Bradham CA, Brenner DA, Baldwin AS Jr, Craven RJ and Cance WG. The focal adhesion kinase suppresses transformation-associated, anchorage-independent apoptosis in human breast cancer cells. Involvement of death receptor-related signaling pathways. *J Biol Chem* 2000; 275: 30597-30604.
- [52] Xu LH, Owens LV, Sturge GC, Yang X, Liu ET, Craven RJ and Cance WG. Attenuation of the expression of the focal adhesion kinase induces apoptosis in tumor cells. *Cell Growth Differ* 1996; 7: 413-418.
- [53] Golubovskaya VM, Zheng M, Zhang L, Li JL and Cance WG. The direct effect of focal adhesion kinase (FAK), dominant-negative FAK, FAK-CD and FAK siRNA on gene expression and human MCF-7 breast cancer cell tumorigenesis. *BMC Cancer* 2009; 9: 280.
- [54] McLean GW, Carragher NO, Avizienyte E, Evans J, Brunton VG and Frame MC. The role of focal adhesion kinase in cancer - a new therapeutic opportunity. *Nat Rev Cancer* 2005; 5: 505-515.
- [55] Cance WG, Kurenova E, Marlowe T and Golubovskaya V. Disrupting the scaffold to improve focal adhesion kinase-targeted cancer therapeutics. *Sci Signal* 2013; 6: pe10.
- [56] Golubovskaya VM, Nyberg C, Zheng M, Kweh F, Magis A, Ostrov D and Cance WG. A small molecule inhibitor, 1,2,4,5-benzenetetraamine tetrahydrochloride, targeting the y397 site of focal adhesion kinase decreases tumor growth. *J Med Chem* 2008; 51: 7405-7416.
- [57] Golubovskaya VM. Targeting FAK in human cancer: from finding to first clinical trials. *Front Biosci (Landmark Ed)* 2014; 19: 687-706.
- [58] Heffler M, Golubovskaya VM, Dunn KM and Cance W. Focal adhesion kinase autophosphorylation inhibition decreases colon cancer cell growth and enhances the efficacy of chemotherapy. *Cancer Biol Ther* 2013; 14: 761-772.

Linc00662 m⁶A promotes PC progression

Supplementary Table 1. The primer sequences for qPCR

Primer		Sequence 5'-3'
β-actin	Forward	TCACCCCACTGTGCCATCTACGA
	Reverse	CAGCGGAACCGCTCATTGCCAATGG
METTL3	Forward	CGTACTACAGGATGATGGCTTTC
	Reverse	TTTCATCTACCCGTTTCATACCC
OIP5-AS1	Forward	TTTGGCACCATTGAAACCA
	Reverse	GCATGGCTACAAATCGACGTA
MAGI2-AS3	Forward	AAGAGCCAGGGACAGCACT
	Reverse	TCTCCAGAACTGGGCTTGTA
AC021078.1	Forward	GATTGATTGGAGTGGGCTAGA
	Reverse	TCCCTCCTCCACCACAAGTA
MIR100HG	Forward	TGTGGCAGAGTAAGGGATGG
	Reverse	CATTGAGGTGGGAAACCAA
Linc00662	Forward	GCAGGAAACAACGAGGATTT
	Reverse	TTTCACGTCAGGCTTCAATG
m6A site 1	Forward	TGCTTTGTGGTGTATGGATTG
	Reverse	ACCTGTTTTCGGTTTTTATTGC
m6A site 2	Forward	GAAGGTGCTTCTGATGTGTG
	Reverse	GGCCAATAATTTTACAGATCA
m6A site 3	Forward	ACAAGTGATCTGTGAAAATAGTTGG
	Reverse	CATGGGATATTCAGTTTTTCACG
m6A site 4	Forward	CATTTCTGAGCCCTTTGAGGC
	Reverse	AATCCTCGTTGTTTCCTGCC
IGF2BP3	Forward	TTGCAGGAATTGACGCTGTA
	Reverse	ACCCAAGGCGTTCAGATTTA
GTF2B	Forward	TTCCTGCTTTCGGTGTGTCT
	Reverse	AACCAAGCCACATTCAGGAC
ITGA1	Forward	GGTACCCTGTGCTGTACCC
	Reverse	CGAAACATTGACTTGGCTGA

Linc00662 m⁶A promotes PC progression

Supplementary Table 2. siRNAs used in this study

siRNA		Sequence 5'-3'
Linc00662 si-1	sense	GGUGUAGGGUAAAUGUUCAACUUCATT
	antisense	UGAAGUUGAACAUUUACCCUACACCTT
Linc00662 si-2	sense	UGACCAU AUGCUGCUUUUACUGUUTT
	antisense	AACAGUAUAAAAGCAGCAU AUGGUCATT
Linc00662 si-3	sense	GAAUUCUCUAGAGCUUUCACAU AATT
	antisense	UUAUGUGGAAAGCUCUAGAGAUUUCTT
IGF2BP3 si-1	sense	CGGUGAAUGAACUUCAGAAUUTT
	antisense	AAUUCUGAAGUUCAUUCACCGTT
IGF2BP3 si-2	sense	GCUGCUGAGAAGUCGAUUACUTT
	antisense	AGUAAUCGACUUCUCAGCAGCTT
IGF2BP3 si-3	sense	GCAGGAAUUGACGCUGUAUAATT
	antisense	UUUAUCAGCGUCAAUUCCUGCTT
GTF2B si-1	sense	CCAAGAGUCACAUGUCCAATT
	antisense	UUGGACAUGUGACUCUUGGAA
GTF2B si-2	sense	CCAUCUCGAGUUGGAGAUUTT
	antisense	AAUCUCCAACUCGAGAUUGGAT
GTF2B si-3	sense	GCUAAUGAUGCUAUAGCUUTT
	antisense	AAGCUAUAGCAUCAUUAGCTC
ITGA1 si-1	sense	GCUCCUCACUGUUGUUCUATT
	antisense	UAGAACAACAGUGAGGAGCTT
ITGA1 si-2	sense	CCUUCUACAUGUUGGACAATT
	antisense	UUGUCCAACAUGUAGAAGGTT
ITGA1 si-3	sense	GGAUGGUAAGACACUGAAATT
	antisense	UUUCAGUGUCUUACCAUCCTT

Supplementary Table 3. The antibodies used in this study

Antibody	Dilution/dose	Supplier (Catalog No.)
METTL3 Rabbit Polyclonal antibody	western blotting 1:1000 immunofluorescence 1:100	Abcam (ab195352)
GTF2B Rabbit Polyclonal antibody	western blotting 1:1000	Abclonal (A1708)
GTF2B Rabbit Monoclonal antibody	RIP 1:20	Abcam (ab109518)
IGF2BP3 Rabbit Polyclonal antibody	western blotting 1:1000 RIP 1:20	Abclonal (A4444)
ITGA1 Rabbit Polyclonal antibody	western blotting 1:1000	Proteintech (22146-1-AP)
GAPDH	western blotting 1:5000	GeneTex (GTX627408)
HRP Goat Anti-Mouse IgG (H+L)	western blotting 1:20000	Abclonal (AS003)
HRP Goat Anti-Rabbit IgG (H+L)	western blotting 1:20000	Abclonal (AS014)
Cy3 Goat Anti-Mouse IgG (H+L)	immunofluorescence 1:150	Abclonal (AS008)
FAK Rabbit pAb	western blotting 1:1000 immunofluorescence 1:100	Abclonal (A11195)
Phospho-FAK-Y397 Rabbit pAb	western blotting 1:1000	Abclonal (AP0302)
Paxillin Rabbit pAb	western blotting 1:1000 immunofluorescence 1:100	Abclonal (A18181)
Phospho-Paxillin-Y118 Rabbit pAb	western blotting 1:1000	Abclonal (AP1156)
Erk1/2 Rabbit mAb	western blotting 1:1000	Abclonal (A4782)
Phospho-ERK1-T202/Y204+ERK2-T185/Y187 Rabbit pAb	western blotting 1:1000	Abclonal (AP0472)